Cell

A Conserved SREBP-1/Phosphatidylcholine Feedback Circuit Regulates Lipogenesis in Metazoans

Amy K. Walker,[1,*] René L. Jacobs,[3] Jennifer L. Watts,[4] Veerle Rottiers,[1,2] Karen Jiang,[1] Deirdre M. Finnegan,[1] Toshi Shioda,[1] Malene Hansen,[5] Fajun Yang,[1,2,7] Lorissa J. Niebergall,[6] Dennis E. Vance,[6] Monika Tzoneva,[4] Anne C. Hart,[1,8] and Anders M. Näär[1,2,*]

[1]Massachusetts General Hospital Cancer Center, Building 149, 13th Street, Charlestown, MA 02129, USA
[2]Department of Cell Biology, Harvard Medical School, Boston, MA 02115, USA
[3]Department of Agricultural, Food and Nutritional Science, 1-32D Ag/For Centre, University of Alberta, Edmonton T6G 2M7, Alberta, Canada
[4]School of Molecular Biosciences, Washington State University, Pullman, WA 99164, USA
[5]The Sanford-Burnham Institute for Medical Research, 10901 North Torrey Pines Road, La Jolla, CA 92037, USA
[6]Department of Biochemistry, University of Alberta, Edmonton T6G 2M7, Alberta, Canada
[7]Present address: Albert Einstein College of Medicine, 1301 Morris Park Avenue, Room 368, Bronx, NY 10461, USA
[8]Present address: Department of Neuroscience, Brown University, 185 Meeting Street, SFH458 Mailbox GL-N, Providence, RI 02912, USA
*Correspondence: amy_walker@mac.com (A.K.W.), naar@helix.mgh.harvard.edu (A.M.N.)
DOI 10.1016/j.cell.2011.09.045

SUMMARY

Sterol regulatory element-binding proteins (SREBPs) activate genes involved in the synthesis and trafficking of cholesterol and other lipids and are critical for maintaining lipid homeostasis. Aberrant SREBP activity, however, can contribute to obesity, fatty liver disease, and insulin resistance, hallmarks of metabolic syndrome. Our studies identify a conserved regulatory circuit in which SREBP-1 controls genes in the one-carbon cycle, which produces the methyl donor *S*-adenosylmethionine (SAMe). Methylation is critical for the synthesis of phosphatidylcholine (PC), a major membrane component, and we find that blocking SAMe or PC synthesis in *C. elegans*, mouse liver, and human cells causes elevated SREBP-1-dependent transcription and lipid droplet accumulation. Distinct from negative regulation of SREBP-2 by cholesterol, our data suggest a feedback mechanism whereby maturation of nuclear, transcriptionally active SREBP-1 is controlled by levels of PC. Thus, nutritional or genetic conditions limiting SAMe or PC production may activate SREBP-1, contributing to human metabolic disorders.

INTRODUCTION

Disorders of metabolism, such as obesity, insulin resistance, and nonalcoholic fatty liver disease (NAFLD), are associated with metabolic syndrome and represent risk factors for more serious diseases such as type II diabetes and cardiovascular disease. However, molecular mechanisms causing dysfunction in these complex diseases remain unclear. The sterol regulatory element-binding protein family (SREBP-1a, -1c, SREBP-2) respond to nutrient levels and regulate transcription of genes required for many aspects of lipid metabolism (Osborne and Espenshade, 2009). SREBP-2 preferentially controls expression of many cholesterogenic genes, whereas SREBP-1 isoforms primarily regulate fatty acid, phospholipid, and triacylglycerol (TAG) biosynthesis genes. In accord with distinct gene regulatory functions, activities of the isoforms appear to be controlled by different regulatory cues. The cholesterol-mediated negative feedback regulation of SREBP-2 is particularly well understood (Brown and Goldstein, 1997). SREBP-2 is produced as an inactive precursor stored with the cholesterol-sensing INSIG/SCAP chaperone complex in the endoplasmic reticulum (ER). Depletion of cholesterol promotes release from INSIG and SCAP-mediated transit of SREBP-2 to the Golgi, followed by proteolytic maturation and nuclear translocation of the transcriptionally active portion to stimulate cholesterogenic gene expression. SREBP-1a and -1c are produced through alternative promoter usage and splicing of the *SREBF1* gene (Horton et al., 2002). Although SREBP-1 isoforms are also synthesized as ER-targeted precursors, SREBP-1c does not appear to be primarily controlled by cholesterol but rather responds to insulin signaling, oxysterols, and feeding cues (Browning and Horton, 2004). In *Drosophila*, palmitate and phosphatidylethanolamine may block processing of the fly SREBP-1 ortholog dSREBP (Dobrosotskaya et al., 2002; Seegmiller et al., 2002) or affect expression of dSREBP target genes in the heart (Lim et al., 2011). However, specific mechanisms linking metabolites from SREBP-1-dependent transcriptional pathways to its maturation as a transcription factor remain unclear.

Invertebrate systems such as *Caenorhabditis elegans* are particularly attractive for determining links between genetics, diet, and metabolism. The *C. elegans* intestine has both digestive and endocrine functions and may model aspects of both hepatic and adipose lipogenesis (Ashrafi et al., 2003). Importantly, the

single ortholog of SREBP in *C. elegans*, SBP-1, appears highly conserved, regulating lipid storage similarly to mammalian SREBP-1 (Horton et al., 2002; McKay et al., 2003). For example, both mammalian SREBP-1 and SBP-1 activate stearoyl-CoA desaturase genes (*SCD* and *fat-6/fat-7*, respectively), requiring the ARC105/MED15/MDT-15 subunit of the Mediator transcriptional coactivator (Yang et al., 2006). We also recently found that both *C. elegans* SBP-1 and mammalian SREBP can be downregulated by the NAD^+-dependent sirtuin SIR-2.1/SIRT1 during fasting (Walker et al., 2010). Thus, the *C. elegans* system is a powerful tool to elucidate conserved gene regulatory mechanisms by SREBP orthologs.

Employing *C. elegans* and mammalian models, we have uncovered a conserved set of SBP-1/SREBP-1 target genes in the one-carbon cycle (1CC), a pathway involving folate-methionine metabolism and manufacture of the predominant methyl donor, *S*-adenosylmethionine (SAMe). Because SAMe is required for the methylation-dependent synthesis of phosphatidylcholine (PC), a key membrane component, regulation of the 1CC by SBP-1/SREBP-1 is consistent with its function in maintaining phospholipid homeostasis (Hagen et al., 2010). Decreased levels of SAMe or PC have been linked to multiple models of hepatosteatosis in rodents and humans; however, mechanisms underlying the strongly elevated lipogenesis have been unclear (Mato et al., 2008; Vance et al., 2007; Vance and Vance, 2004; Zeisel, 2008). Our observations indicate that an important regulatory mechanism for SREBP-1 activation may operate when methylation capacity or PC biogenesis is diminished and suggest that this pathway may contribute to lipid accumulation in fatty liver disease.

RESULTS

SREBPs Regulate 1CC Genes in *C. elegans* and in Mammalian Cells

The SREBP family of transcription factors regulates genes involved in biosynthesis and trafficking of cholesterol and other lipids in mammals (Osborne and Espenshade, 2009). Employing the nematode *C. elegans* to elucidate conserved functions associated with SREBP regulation in metazoans, we have carried out genome-wide gene expression analysis on worms depleted of the single SREBP ortholog SBP-1. As expected, the DNA microarray studies showed that expression of many genes important for fatty acid, TAG, and phospholipid production is dependent on SBP-1 (Figure 1A and Figure S1A available online). Intriguingly, our analysis also found enrichment of genes predicted to function in the one-carbon cycle (1CC) (Figures 1A–1C). The 1CC coordinates folate and methionine metabolism with production of the methyl donor *S*-adenosylmethionine (SAMe) (Mato and Lu, 2005). SAMe is critical for most cellular methylation reactions, including methylation-dependent synthesis of a large number of cellular metabolites and phospholipids (Mato et al., 2008). Because of the central importance of the 1CC to metabolic homeostasis, we examined regulation of the 1CC by SBP-1/SREBP in more detail. Analysis of individual 1CC genes identified in DNA microarray studies, as well as closely related genes, by quantitative RT-PCR (qRT-PCR) after *sbp-1* RNAi confirmed that a broad array of 1CC genes depend on SBP-1 for full expression (Figure 1C).

Because 1CC genes had not been identified in previous searches for mammalian SREBP target genes, we also examined their regulation in human cells. We found that overexpression of SREBP-1a in human embryonic kidney 293T cells resulted in upregulation of multiple 1CC genes (Figure 1D). Several of these, such as *CTH* and *MAT1A,* are orthologs of genes identified in our *C. elegans* studies, whereas others, such as *CBS*, appeared specific to regulation in mammalian cells. We also found that expression of *MAT1A* specifically depended on SREBPs in human cells, whereas *MAT2A* did not (Figure S1B). This suggests that SREBP regulation of 1CC genes is conserved among metazoans and that metabolic flux through this pathway may be controlled by SREBP orthologs.

Increased SBP-1-Dependent Lipogenesis and Gene Expression after *sams-1* Depletion in *C. elegans*

To better understand the link between methyl donor homeostasis and regulation of these genes by SBP-1, we examined phenotypes of nematodes depleted for the SAMe synthase-encoding gene *sams-1*. The *sams-1* gene was initially identified in an RNAi screen for extended *C. elegans* life span (Hansen et al., 1995). Surprisingly, we find that nematodes depleted or mutated for *sams-1* (*sams-1(RNAi)* and *sams-1(lof)*, respectively) also exhibit large refractile droplets within the intestine and body cavity that stained with Sudan Black (Figures 2A–2C), suggesting that lipid accumulation was increased. Accordingly, we found that TAGs in *sams-1(RNAi)* nematodes were significantly elevated when compared to controls (Table 1). Although *C. elegans* harbor four additional *sams* genes, RNAi of *sams-1* resulted in an approximately 65% decrease in SAMe levels, with similar decreases in *S*-adenosylhomocysteine (SAH), the product of SAMe-dependent methyltransferase reactions (Figure 2D). This suggests that *sams-1* is required for the majority of global SAMe production in *C. elegans* under normal growth conditions. The lipid accumulation seen after *sams-1* RNAi led us to hypothesize that low methylation capacity may feedback activate SBP-1 and promote increased lipogenesis, akin to the classical feedback activation of mammalian SREBP-2 in response to low cholesterol.

To determine whether decreased methylation capacity could affect nuclear SBP-1 levels and promote elevated lipogenesis, we examined cellular localization of a GFP::SBP-1 fusion protein and SBP-1-dependent transcription of lipogenic genes in *sams-1(RNAi)* nematodes. Indeed, GFP::SBP-1 showed increased nuclear accumulation after *sams-1* RNAi (Figure 2E), suggesting that levels of transcriptionally active SBP-1 are increased. Concomitantly, expression of multiple SBP-1-dependent genes, including the palmitoyl-CoA desaturase *fat-5* and the stearoyl-CoA desaturases *fat-6* and *fat-7*, were increased in both *sams-1(RNAi)* and *sams-1(lof)* animals (Figures 2F and S2A). Similar levels of *sbp-1* mRNA were present in control, *sams-1(lof)*, and *sams-1(RNAi)* nematodes, showing that regulation of SBP-1 in response to SAMe depletion is likely posttranscriptional (Figure S2A; data not shown). To determine whether SBP-1 was necessary for increased lipogenic gene expression after *sams-1* RNAi, we examined *sams-1* knockdown phenotypes in nematodes expressing a hypomorphic *sbp-1* allele (*sbp-1(ep79)*). Elevated expression of *fat-5, fat-6*, and *fat-7*, or the characteristic

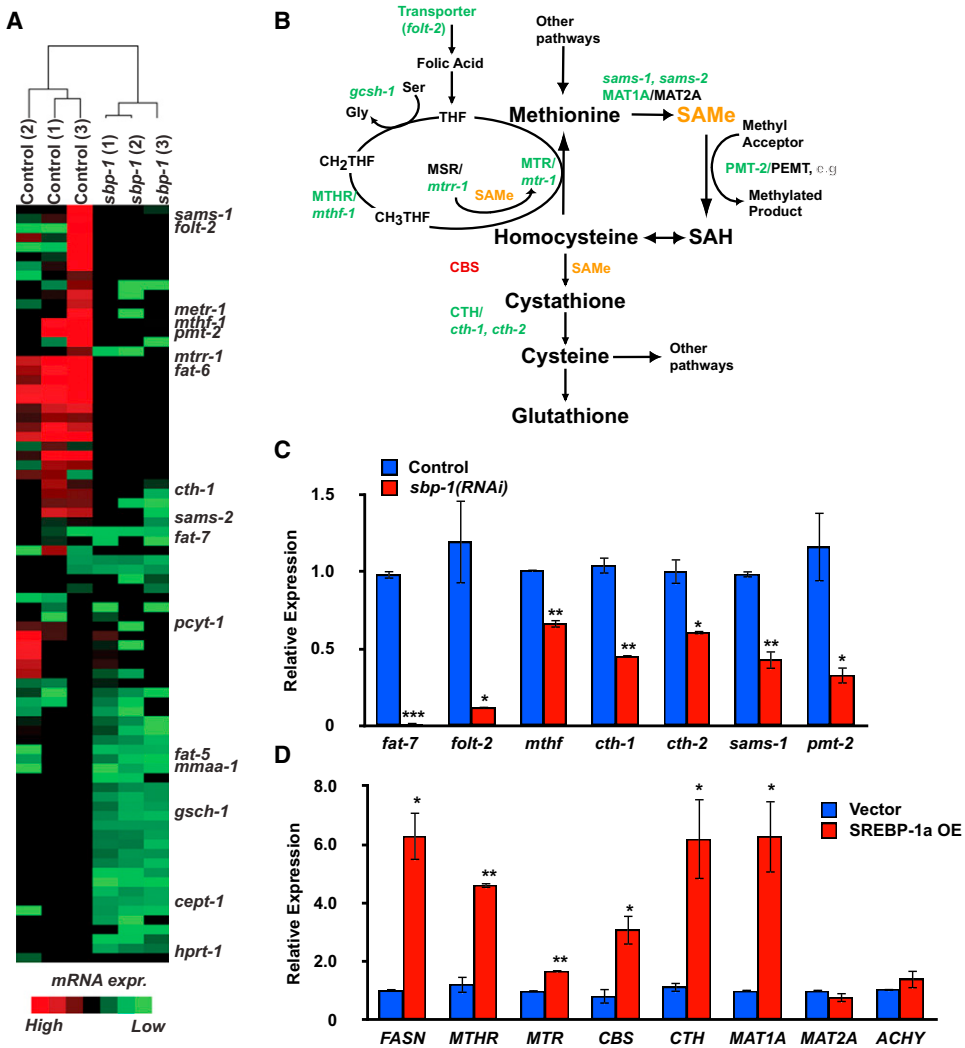

Figure 1. Coregulation of One-Carbon Cycle and Fatty Acid Biosynthesis Genes by SBP-1/SREBP-1

(A) Unbiased hierarchical clustering of genes more than 2-fold downregulated in *sbp-1(RNAi)* nematodes and with metabolic regulation KEGG terms shows that one-carbon cycle (1CC) genes are decreased similarly to known SBP-1-responsive genes in lipid metabolism.

(B) Schematic diagram of the one-carbon cycle (1CC). SBP-1-dependent genes in *C. elegans* are shown in green; genes responsive to mammalian SREBP-1 are shown in red.

(C) Quantitative RT-PCR (qRT-PCR) from control or *sbp-1(RNAi)* nematodes reveals that multiple 1CC genes require SBP-1 for expression.

(D) qRT-PCR from 293T cells overexpressing SREBP-1a shows that expression of multiple 1CC genes increases with elevated SREBP-1 activity.

Error bars show SD. Statistical relevance (p value) shown by < 0.05, *; < 0.01, **; < 0.005, ***. See also Figure S1.

lipid droplets, was not observed when both *sams-1* and *sbp-1* function were limited (Figures 2F and S2B), suggesting that SBP-1 is essential for increased lipogenesis after *sams-1* depletion.

Decreased Phosphatidylcholine Production in *C. elegans* Is Linked to Elevated SBP-1-Dependent Gene Expression and Lipogenesis after *sams-1* RNAi

We next examined whether depletion of *sams-1* caused specific metabolic changes that might be linked to increases in SBP-1 activity. Intriguingly, methylation-dependent phosphatidylcholine (PC) biogenesis intermediates were altered in metabolomic analysis of *sams-1*-depleted nematodes (Figures 3B and 3C). PC is produced by two alternative pathways. It can be synthesized either from choline (Kennedy pathway) or by methylation of phosphatidylethanolamine (PE) by PEMT in mammals, or of phosphoethanolamine by PMT-1 and PMT-2 orthologs in *C. elegans* and plants (Figure 3A) (Brendza et al., 2007; Palavalli et al., 2006; Vance and Vance, 2004). In accord with the critical role of methylation for the production of PC, we found significantly lower levels of phosphocholine, the product of the PMT-1 methyltransferase (Figure 3B), as well as dramatically decreased PC levels, after *sams-1* RNAi, whereas PE was not significantly changed (Figure 3C). Thus, marked alterations in phospholipid

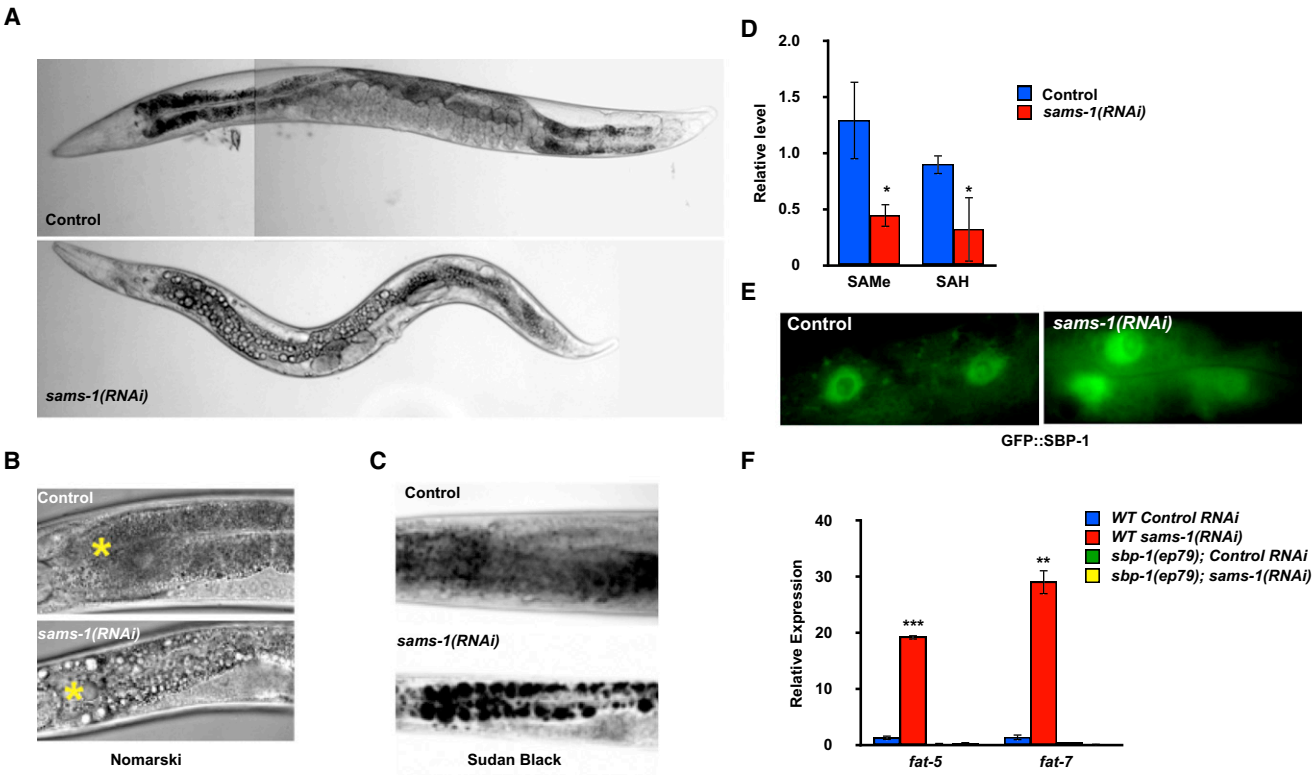

Figure 2. In *C. elegans*, SBP-1-Dependent Lipogenesis and Gene Expression Are Increased after *sams-1(RNAi)*

(A) RNAi knockdown of *sams-1* revealed large refractile droplets in the intestine and body cavity by Nomarski optics.

(B) Enlarged view of droplets by Nomarski optics. The first sets of intestinal cells are shown, and the position of the pharynx is marked with a yellow star.

(C) Staining with Sudan Black shows that droplets in *sams-1(RNAi)* nematodes contain lipids.

(D) SAMe and SAH levels are significantly decreased after *sams-1(RNAi)*. Error bars represent SEM between triplicate independent experiments.

(E) Nuclear accumulation of a GFP::SBP-1 fusion protein is increased in *sams-1(RNAi)* intestinal cells.

(F) qRT-PCR comparing levels of *fat-5* and *fat-7* in wild-type or a hypomorphic *sbp-1* allele (*ep79*) demonstrated that FA desaturase upregulation in *sams-1(RNAi)* animals depends on *sbp-1*.

Error bars show SD. Statistical relevance (p value) shown by < 0.05, *; < 0.01, **, < 0.005, ***. See also Figure S2.

metabolism occur along with increased lipogenesis in *sams-1(RNAi)* nematodes. Similar to our observation in *sams-1*-deficient nematodes, accumulation of large lipid droplets has been associated with low PC levels or changes in PC/PE ratios in *Drosophila* and mammalian models (Guo et al., 2008; Jacobs et al., 2008; Li et al., 2006). We therefore wished to determine whether this increased lipid droplet formation might be linked mechanistically to increased SBP-1/SREBP-1 activity.

Table 1. Increased Triacylglycerols in *sams-1*, *pcyt-1*, or *cept-1(RNAi)* Nematodes

	%TAG	SEM	p value
Control	42.8	2.6	
sams-1(RNAi)	64.5	4.1	0.0024
pcyt-1(RNAi)	51.4	1.6	0.0401
cept-1(RNAi)	50.8	1.6	0.0801

Quantitative analysis demonstrates increased storage of neutral lipids after RNAi knockdown of genes necessary for PC production in nematodes when comparing percent triacylglycerol (TAG) to total lipids. SEM is standard error of the mean.

Production of PC from either phosphoethanolamine or PE requires three sequential SAMe-dependent methylation steps; however, PC synthesis from choline by the Kennedy pathway is methylation independent (Vance and Vance, 2004). To determine whether rescuing PC production would reverse SBP-1-dependent lipogenic events in *sams-1(RNAi)* nematodes, we provided excess dietary choline. Strikingly, dietary choline supplementation completely rescued accumulation of lipid droplets and corrected overexpression of the SBP-1 transcriptional targets *fat-5*, *fat-6*, and *fat-7* in *sams-1(RNAi)* worms (Figures S3A and S3B; data not shown). These results support our hypothesis that decreased levels of PC in *sams-1(RNAi)* worms may be directly linked to the increased SBP-1-dependent lipogenesis.

Defective PC Production Results in Increased SBP-1-Dependent Gene Expression and Lipogenesis in *C. elegans*

Although decreased methylation capacity prevents adequate PC synthesis, lowering levels of SAMe could also affect a broad array of methyltransferases. We next wished to address the

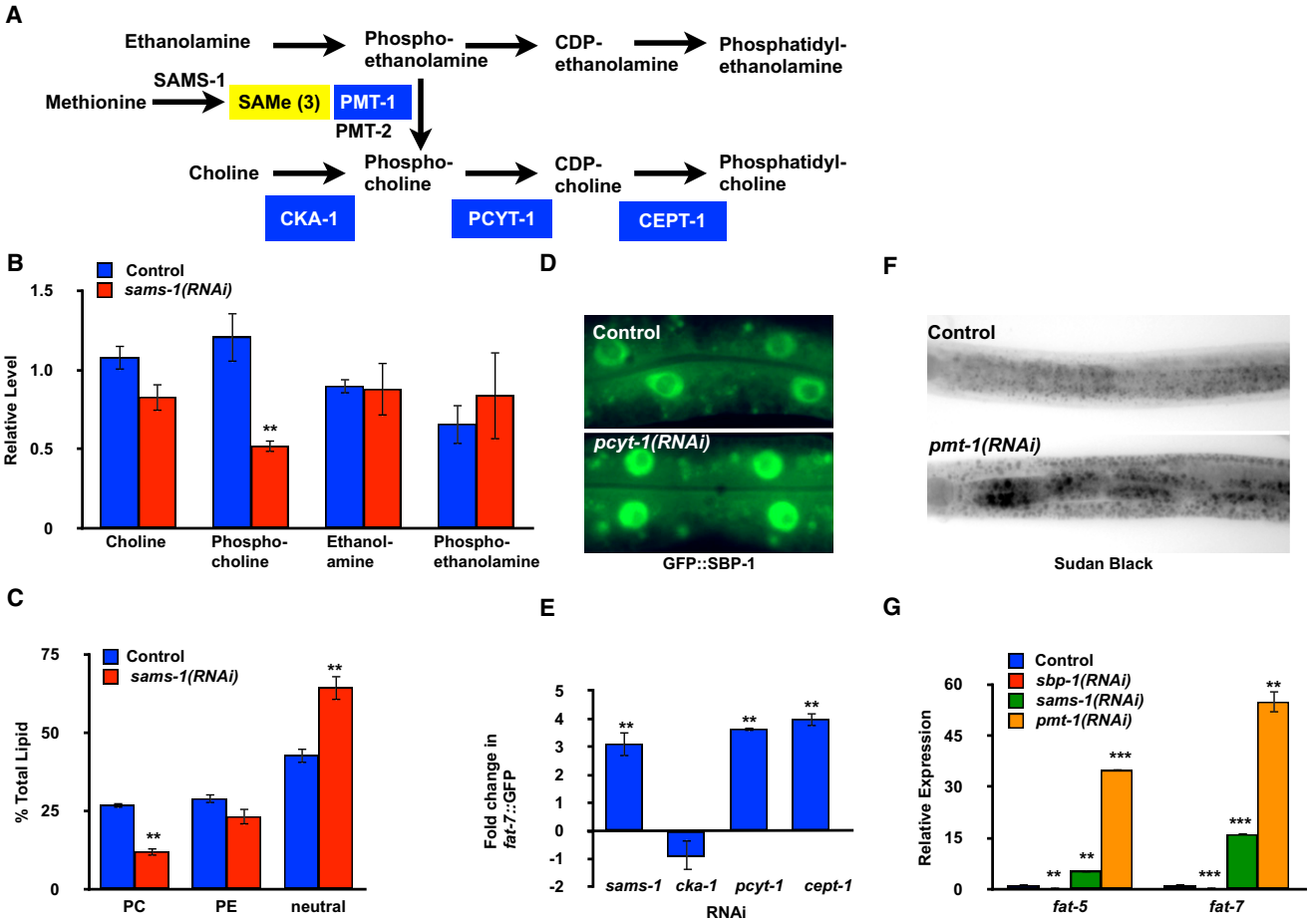

Figure 3. Increased Lipogenesis and SBP-1-Dependent Gene Expression after *sams-1* RNAi in *C. elegans* Are Linked to Limited Phosphatidylcholine Production

(A) Schematic diagram of links between methyl production and phospholipid biosynthesis in nematodes. Enzymes whose functions are disrupted by RNAi in subsequent panels are shown in blue boxes.

(B) Analysis of metabolites in *sams-1(RNAi)* nematodes shows that PC precursors downstream of methylation steps are decreased (phosphocholine), whereas metabolites upstream (choline, ethanolamine, phosphoethanolamine) are unchanged or slightly increased. Error bars represent SEM between quadruplicate independent experiments.

(C) Quantitative analysis shows that PC levels are diminished after *sams-1(RNAi)*. Error bars represent SEM between quadruplicate independent experiments.

(D) GFP::SBP-1 accumulates in intestinal nuclei after *pcyt-1(RNAi)*.

(E) Quantitative measurement of *pfat-7*::GFP intensity in *C. elegans* populations by a COPAS biosorter shows that RNAi knockdown of PC biosynthesis genes downstream of methylation steps activate this SBP-1-dependent reporter at similar levels to *sams-1* RNAi.

(F and G) Blocking methylation-dependent PC production by interference with PMT-1 produces similar phenotypes to *sams-1(RNAi)*, such as increased lipid droplet formation (F) and overexpression of SBP-1 transcriptional targets, *fat-5* and *fat-7* (G).

Error bars show SD; statistical relevance (p value) shown by < 0.05, *; < 0.01, **, < 0.005, ***. See also Figure S3 and Table S1.

question of whether limiting PC levels are specifically associated with SBP-1-dependent lipogenesis and lipid droplet formation in *C. elegans*. Indeed, RNAi knockdown of *pcyt-1* or *cept-1*, encoding the final enzymes in the PC biosynthesis pathway (Figure 3A), resulted in decreased PC levels, elevated nuclear localization of GFP::SBP-1, and increased stored lipids, similar to what we observed in *sams-1(RNAi)* nematodes (Figure 3D, Table 1, Table S1, and data not shown). Furthermore, in an independent, unbiased screen (V.R. and A.M.N., unpublished data), we found that RNAi of genes involved in SAMe production or genes encoding enzymes acting downstream of the methylation step in PC biogenesis resulted in strong upregulation of a GFP reporter fused to the promoter of the SBP-1 target gene *fat-7* (*pfat-7*::GFP) (Figure 3E). By contrast, RNAi of *cka-1*, encoding a choline kinase upstream of the methylation-dependent PC synthesis step, did not increase *pfat-7*::GFP expression (Figure 3E). We also examined lipid accumulation and expression of SBP-1 target genes after knockdown of *pmt-1*, encoding the PMT-1 phosphoethanolamine methyltransferase, a key consumer of SAMe during PC production in *C. elegans*. Reduction of *pmt-1* expression causes a late larval arrest and defects in PC production that can be rescued by dietary choline

supplementation (Brendza et al., 2007). We also found that *pmt-1* knockdown increased lipid droplet formation and caused a marked elevation in expression of the SBP-1-responsive genes *fat-5* and *fat-7* (Figures 3F and 3G). Although limitation of SAMe production could cause pleiotropic phenotypes by reducing activity of various distinct methyltransferases, the similar effects of *sams-1* or *pmt-1* depletion on SBP-1-dependent gene expression and lipogenesis suggest that reduced production of PC is directly affecting SBP-1 activity.

Activation of ER Stress Response in *sams-1(RNAi)* Animals Is Not Linked to Elevated SBP-1-Dependent Lipogenic Gene Expression

Because the decrease in PC levels tightly correlates with increased SBP-1 activity, we hypothesized that lowered PC in intracellular membranes could alter proteolytic processing and maturation of SREBP-1 orthologs. ER stress may be sufficient to initiate SREBP processing in mammals, independent of the cholesterol feedback cycle (Ferré and Foufelle, 2010). Therefore, we asked whether *sams-1* depletion could promote ER stress responses and whether such activation would be sufficient to upregulate SBP-1-dependent gene expression. In *C. elegans*, the BiP/GRP78 ortholog *hsp-4* is induced by ER stressors such as the glycosylation inhibitor tunicamycin and depends on the activity of the ER stress effector XBP-1 (Calfon et al., 2002). RNAi of *sams-1* in a *hsp-4*::GFP reporter line shows a strong *xbp-1*-dependent increase in GFP expression (Figure S3C), suggesting that ER stress responses are robustly activated in these animals. To determine whether ER stress response was functionally important for the elevated SBP-1 activity observed after loss of *sams-1*, we knocked down the ER stress effectors *atf-6* or *ire-1* (Shen et al., 2005) in *sams-1(lof)* nematodes and found that SBP-1 target gene upregulation and lipid droplet accumulation were not altered (Figure S3D; data not shown). Next we asked whether cellular responses to ER stress could activate SBP-1 in wild-type animals and found that SBP-1 target gene expression was not affected by doses of tunicamycin causing mild or moderate levels of lethality in control cultures (Figure S3E; data not shown). Although our results point to a significant activation of ER stress responses when *sams-1* is depleted, ER stress does not appear to cause increased SBP-1-dependent gene expression and lipogenesis.

Increase in Mammalian SREBP-1 Nuclear Localization and Lipid Droplet Size after Blocking PC Biogenesis in Human Hepatoma Cells

Our *C. elegans* results suggest that SBP-1 activity increases in *sams-1(RNAi)* nematodes as methylation capacity is diminished, and that mechanisms underlying this phenomenon are directly related to decreased PC levels. In order to determine whether mammalian SREBP-1 might also be regulated by PC depletion, we used short-interfering (si) RNA technology to inhibit expression of genes necessary for PC production in human cells. As in invertebrates, PC production in mammals may proceed through methylation-dependent or -independent pathways, although in mammals PE is methylated to generate PC (Figure 4A) (Vance and Vance, 2004). We found that blocking PC production through siRNA-mediated depletion of enzymes in the methylation-dependent steps (*MAT1A, PEMT*) or enzymes in the methylation-independent CDP-choline pathway (*CTα, CEPT*) in human HepG2 hepatoma cells resulted in increased accumulation of large lipid droplets, akin to our observations in *C. elegans* (Figures 4B, 4D, 4F, S4E, data not shown). These data are in accord with the development of fatty liver in *Mat1a*- (Lu et al., 2001), *Ctα*-, and *Pemt*-deficient mice on a high-fat diet (Jacobs et al., 2008, 2010; Watkins et al., 2003) and with accumulation of lipid droplets in cell culture models that limit PC production (Guo et al., 2008; Jacobs et al., 2008; Testerink et al., 2009). Our results reveal that along with increases in lipid droplet size, HepG2 cells depleted of *CTα*, *CEPT*, *MAT1A*, or *PEMT* showed SREBP-1 concentrated in the nucleus in immunofluorescence assays (Figures 4C, 4E, S4B, and S4C), whereas controls exhibited stronger staining in the cytoplasm, where the inactive SREBP-1 precursor is stored. Furthermore, qRT-PCR of *CTα* knockdown cells showed increased expression of SREBP-1 transcriptional targets *SCD1* and *MAT1A* but no increases in the expression of *SREBF1* gene encoding the SREBP-1 protein (Figure 4F), suggesting that elevation of SREBP-1 activity is likely posttranscriptional. As in our *C. elegans* studies, these experiments suggest that limitation of PC biosynthesis in mammalian cells promotes elevated levels of nuclear SREBP-1, resulting in increased SREBP-1-dependent gene expression, and in elevated lipogenesis and lipid droplet formation.

In contrast with potent effects of PC limitation on SREBP-1 nuclear accumulation, nuclear levels of SREBP-2, which regulates genes for cholesterol biosynthesis (Osborne and Espenshade, 2009), were already high in control cells and did not increase when PC synthesis was blocked by siRNA of *CTα*, *CEPT*, *MAT1A*, or *PEMT* (Figures 4G and S4D; data not shown). Because strong nuclear accumulation of SREBP-2 is likely due to low levels of cholesterol in our culture conditions, which could mask additional effects from decreased PC, we also compared SREBP-1 and SREBP-2 nuclear accumulation in the presence of cholesterol. We found that SREBP-1 was preferentially nuclear in *CTα* and *CEPT* knockdown cells regardless of cholesterol levels (Figures 4E, S4B, and S4C). However, nuclear levels of SREBP-2 were high in low cholesterol and then decreased when cholesterol was added, whether in control, *CTα*, or *CEPT* knockdown cells (Figures 4G and S4D). This suggests that under these culture conditions, blocking PC synthesis has a greater effect on SREBP-1 nuclear accumulation, gene expression, and lipogenesis, and that SREBP-2 responds preferentially to cholesterol levels.

Decreased PC Biosynthesis in Murine Liver Promotes SREBP-1 Proteolytic Maturation and Target Gene Expression

To determine whether inhibition of PC biosynthesis in a mammalian in vivo model also altered SREBP-1 processing and target gene expression, we examined livers from mice deficient in PC biosynthesis due to a liver-specific deletion in *Ctα*, encoding the rate-limiting enzyme in PC biosynthesis from choline (Vance and Vance, 2004) and the ortholog to *C. elegans pcyt-1*. Livers from $Ct\alpha^{-/-}$ mice on a high-fat diet exhibit decreased PC and increased TAG compared to controls but have normal

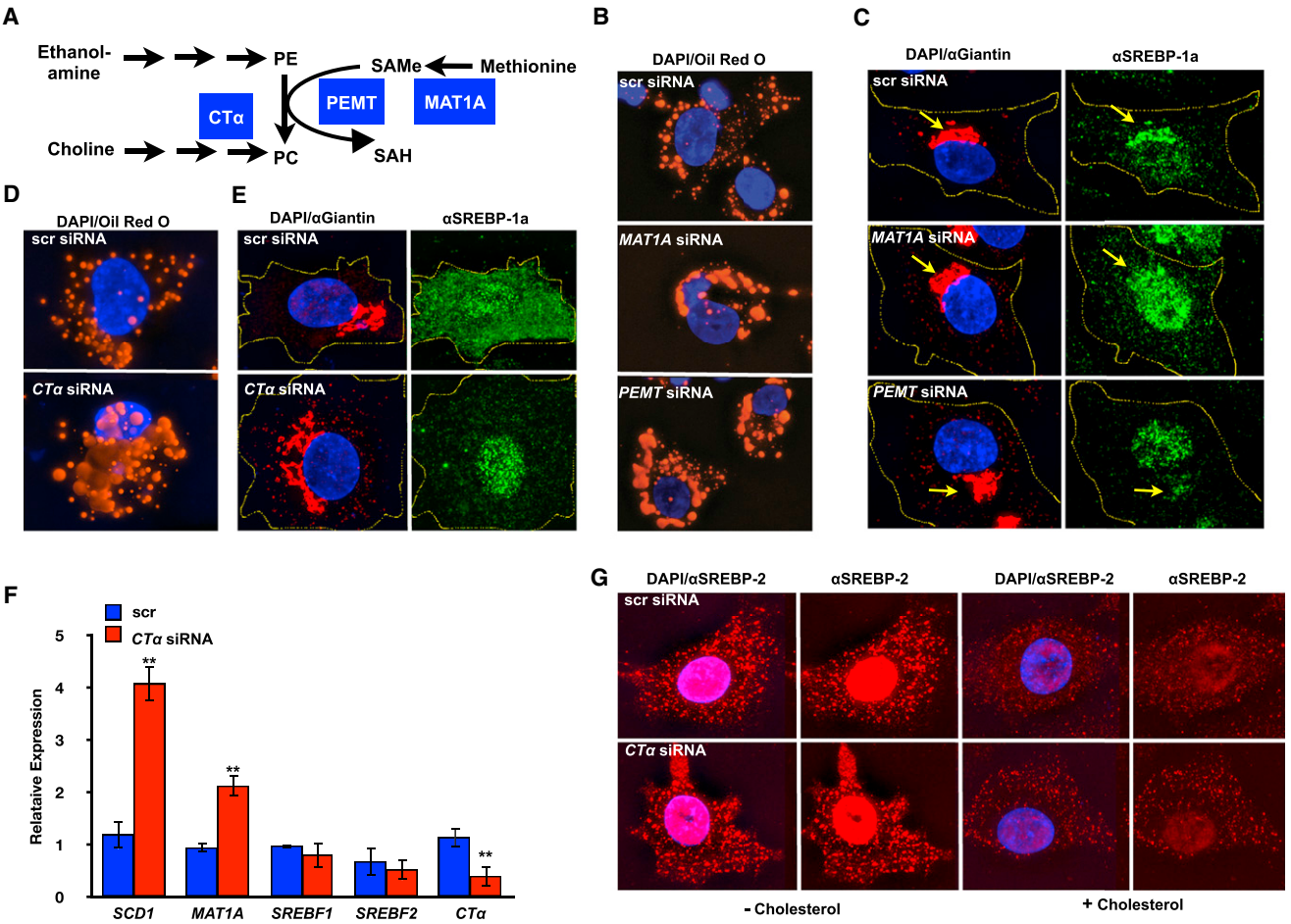

Figure 4. Increase in Lipid Droplet Formation and SREBP-1a Nuclear Localization in Human Hepatoma Cells in Response to SAMe/PC Depletion

(A) Schematic diagram of links between mammalian methyl production and phospholipid biosynthesis. Enzymes whose functions are disrupted by siRNA in subsequent panels are shown in blue boxes.

(B–E) siRNA knockdown of *PEMT*, *MAT1A* (B), or *CTα* (D) causes increased accumulation of large lipid droplets by Oil Red O staining in HepG2 cells in lipid-depleted serum. Immunostaining with an antibody against SREBP-1a shows increased nuclear accumulation after *PEMT, MAT1A* (C), or *CTα* (E) knockdown. Cells were costained with antibodies recognizing the Golgi marker Giantin. Yellow lines show outline of cells.

(F) Analysis of gene expression in *CTα* knockdown HepG2 cells by qRT-PCR shows increases in SREBP-1-dependent genes such as *SCD1* and *MAT1A*. Error bars show SD. Statistical relevance (p value) is shown by <0.05, *; <0.01, **, <0.005, ***.

(G) Antibodies directed against SREBP-2 were used to stain HepG2 cells in lipid-depleted serum in the presence or absence of 10 μg/ml cholesterol in control or *CTα* siRNA-treated cells.

See also Figure S4.

cholesterol levels (Jacobs et al., 2004). To determine whether SREBP function was altered, we examined SREBP-1 and SREBP-2 in extracts from $Ct\alpha^{-/-}$ livers by immunoblotting and found higher levels of mature, processed SREBP-1 (Figures 5A and 5B), suggesting that lowering PC is sufficient to affect mammalian SREBP-1a/c proteolytic maturation. In accord with our findings in *C. elegans*, expression of the Δ9 fatty acid desaturase and key lipogenic SREBP-1 target gene *Scd1* (orthologous to *fat-6 and fat-7*) was increased in livers from $Ct\alpha^{-/-}$ mice (Figure 5C). Previous studies of $Ct\alpha^{-/-}$ mice did not uncover changes in *Scd1* expression, probably because of the use of fasted mice (Jacobs et al., 2004), a condition known to strongly inhibit SREBP target gene expression (Horton et al., 1998; Walker et al., 2010). As previously reported (Jacobs et al., 2005), expression of the *sams-1* ortholog *Mat1a* is also upregulated in these livers. However, we found that levels of mature SREBP-2 and expression of SREBP-2 target genes were not increased in $Ct\alpha^{-/-}$ livers, and that there were no increases in the expression of the *Srebf1a/c* and *Srebf2* genes themselves (Figures 5C–5E). This in vivo study suggests that, as in our cell culture studies, SREBP-2 activity may not be significantly affected in response to altered PC levels, whereas processed, mature SREBP-1 is increased, along with SREBP-1-dependent transcription and concomitant lipogenesis.

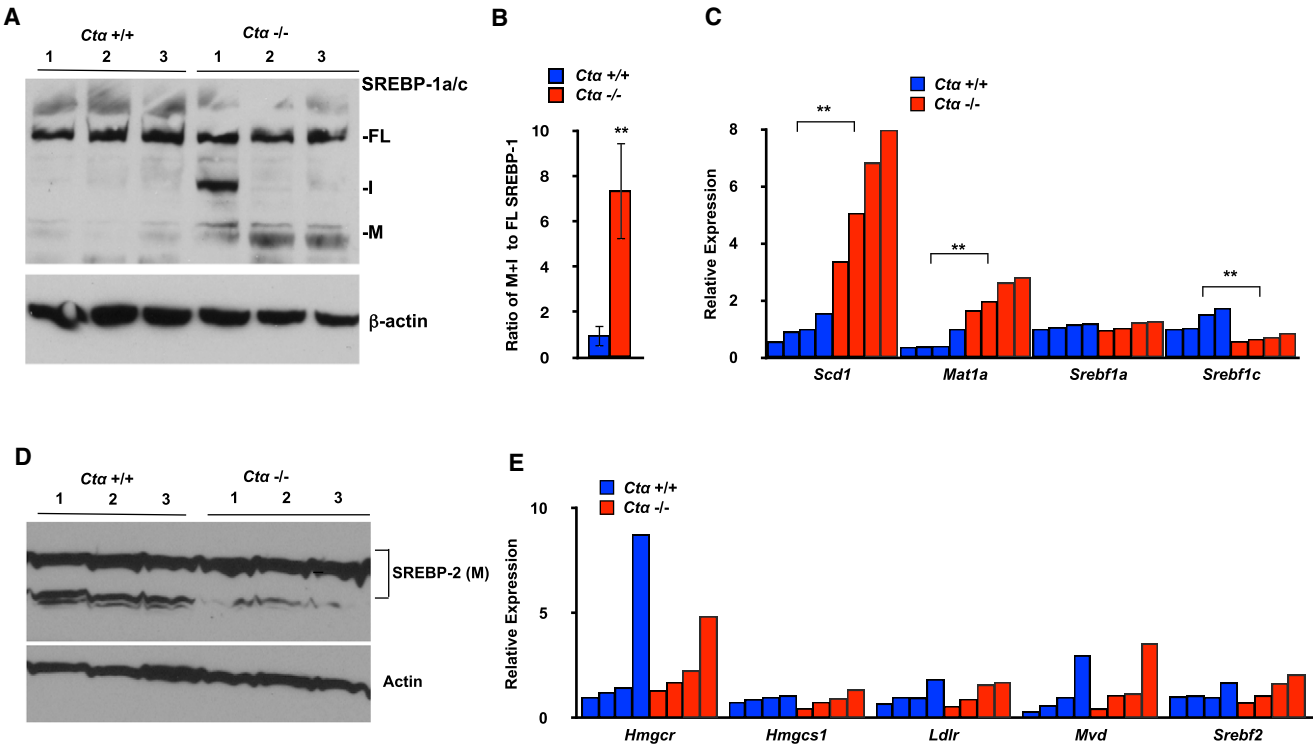

Figure 5. Increase in SREBP-1 Processing and Target Gene Expression in *Ctα* Knockout Mouse Livers

(A) Immunoblotting of extracts from mice with a liver-specific knockout of *Ctα* (Jacobs et al., 2004) limiting the CDP-choline pathway shows increased SREBP-1a/c processing (Jacobs et al., 2004). Fl is full-length SREBP-1a/c precursor; I, intermediate form; M, mature, transcriptionally active form.

(B) Analysis of the immunoblot by densitometry shows increases in proteolytic products of SREBP-1 in livers from *Ctα* knockout mice. Error bars show SD. Statistical relevance (p value < 0.01) is shown by **.

(C) Analysis of gene expression by qRT-PCR from *Ctα* knockout mice shows increased expression of *Scd1*, an SREBP-1 target, as well as *Mat1a*, ortholog of *sams-1*. Bars represent individual mice; error bars show SD; statistical relevance (p value < 0.01) shown by (**).

(D and E) Analysis of gene expression by qRT-PCR from the liver-specific *Ctα* knockout mice (Jacobs et al., 2004) shows no statistically significant changes in levels of mature, processed SREBP-2 (D) or target gene expression (E). Bars represent individual mice; error bars show SD; statistical relevance (p value < 0.01) shown by (**).

Inhibition of PC Biosynthesis Affects Localization of SREBP-Activating Proteases and Parallels Inactivation of ARF-GTPases Regulating COPI Golgi-ER Retrograde Transport

Our results indicate that lipogenic SREBPs (SBP-1/SREBP-1) exhibit increased activity when PC synthesis is limited. This regulation occurs in the presence of cholesterol, suggesting that it represents an independent mechanism to regulate SREBP-1. Therefore, we examined the dependence of this regulatory circuit on SCAP, the cholesterol-binding chaperone essential for the classical feedback pathway controlling SREBP-2 processing and maturation (Brown and Goldstein, 1997). RNAi-mediated depletion of *Ctα* in SRD13A cells, in which SCAP is mutated and inactivated (Hua et al., 1996), resulted in robust nuclear accumulation of SREBP-1 (Figures 6A and S5A), suggesting that the mechanism activating SREBP-1 in response to PC depletion is indeed distinct from the classical pathway involving SCAP-dependent transfer of SREBPs from the ER to the Golgi when cholesterol is limiting.

Because PC is a major membrane component, and SREBP-1 activation occurs within the confines of the ER and Golgi membranes, we hypothesized that changes in these membranes could lead to increased SREBP-1 activity. The balance of PC/PE ratio affects membrane fluidity and curvature, and depletion of PC can alter protein trafficking and lipid accumulation (Hagen et al., 2010; Testerink et al., 2009). The antibiotic brefeldin A (BFA) inactivates the ARF-GTPase cycle critical for regulation of COPI or retrograde protein transport from the Golgi apparatus to the ER (Donaldson and Lippincott-Schwartz, 2000). BFA has also been reported to disrupt localization of the Golgi-resident SREBP-activating Site-1 and Site-2 proteases (S1P, S2P), causing ectopic proteolytic cleavage of SREBP-2 in the ER (DeBose-Boyd et al., 1999). We asked whether decreased PC levels could similarly affect S1P and S2P localization to induce SREBP-1a processing and nuclear accumulation. Interestingly, when *CTα* or *CEPT* were depleted in HepG2 cells, S1P and S2P lost Golgi-specific localization and appeared instead in a diffuse cytoplasmic pattern consistent with KDEL ER-marker staining (Figures 6B, 6C, and S5B–S5D; data not shown). Indeed, localization of two additional Golgi-specific proteins, Giantin and α-mannosidase, was also disrupted (Figures 4C, 4E, 6B, 6C, S5B, and S5C),

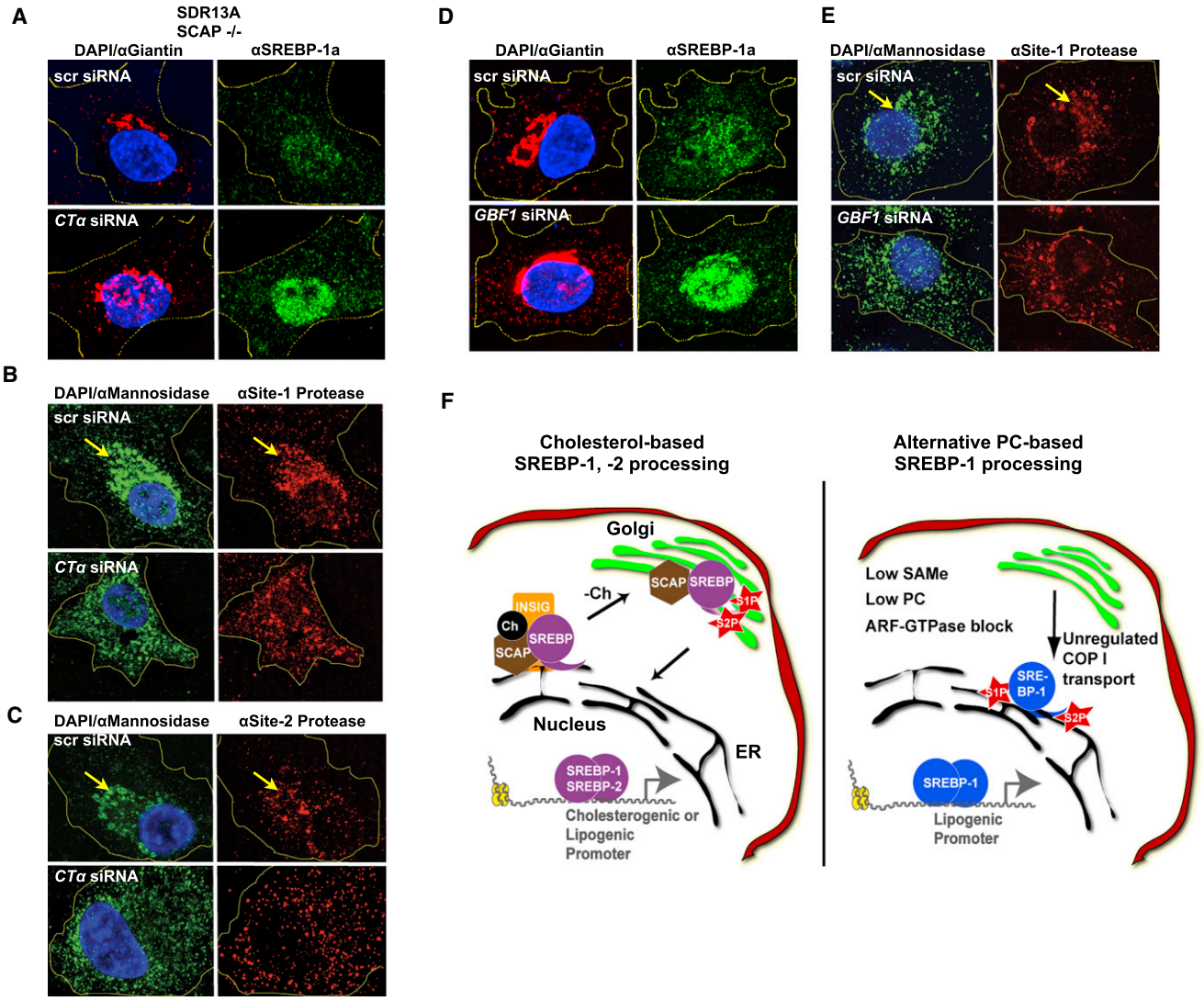

Figure 6. Relocalization of SREBP-Activating Proteases in Mammalian Cells when PC Production Is Blocked

(A) SREBP-1 accumulates in the nucleus after *CTα* siRNA treatment in SRD13A cells, which lack a functional SCAP. Yellow lines show cell outlines.

(B and C) Coimmunostaining of HepG2 cells with the Golgi marker α-mannosidase and antibodies to S1P (B) or S2P (C) shows a strong shift away from an organized Golgi structure and disorganization of SREBP-activating protease staining after *CTα* knockdown. Yellow arrow marks Golgi body in control cells.

(D and E) Interference with ARF-GTPase signaling by GBF1 siRNA treatment of HepG2 cells increases SREBP-1 nuclear accumulation (D) and disrupts Golgi-specific partitioning of S1P (E).

(F) Schematic model for relocalization of SREBP-activating proteases, resulting in activation of SREBP-1 and transit to the nucleus upon decreased SAMe or PC levels or blocks in ARF-GTPase cycles.

See also Figure S5.

suggesting the Golgi may be broadly affected by changes in PC levels.

Recent studies have found that the ARF-activating protein/GEF GBF1 affects S2P localization in the unfolded protein response (Citterio et al., 2008). To gain further insights into ER-Golgi trafficking of SREBP-activating proteases, we used siRNA to deplete GBF1 and found increases in SREBP-1 nuclear accumulation and redistribution of S1 and S2 proteases to an ER-like pattern, similar to the effects of PC depletion (Figures 6D, 6E, S5E, and S2F). ARF signaling may also be inhibited by increases in membrane curvature (Bigay et al., 2003), which are predicted to occur when membrane PC levels drop (Lev, 2006). Thus, SREBP-1 nuclear accumulation could occur if PC levels drop and membrane curvature inhibits ARF-GTPase signaling, allowing relocalization of S1P and S2P to the ER and proteolytic activation of SREBP-1 (Figure 6F). Limitations in choline or methionine metabolism affecting PC synthesis could activate SREBP-1 through this mechanism, promoting the lipid accumulation in fatty liver disease.

DISCUSSION

Regulation of SBP-1/SREBP-1 Activity by Phospholipids

Studies by a number of groups have revealed a complex regulatory relationship between SREBPs and phospholipids. SREBP-1a has been implicated as a regulator of phospholipid biogenesis genes in mammals (Hagen et al., 2010), and we have found that multiple PC biosynthesis genes are dependent on SBP-1 in *C. elegans* (Figures 1A, 1B, and S1A). In a *Drosophila* cell culture model, Dobrosotskaya et al. showed that palmitate and precursors to PE are potent inhibitors of dSREBP processing (Dobrosotskaya et al., 2002). However, genes or metabolites leading directly to PC biosynthesis were not examined. The differences in our studies may reflect a distinct SREBP-regulatory circuit in *Drosophila*, or perhaps that specific combinations of membrane phospholipids may differently affect SREBP processing. Nevertheless, a recent study showed that low PE levels in the *Drosophila* heart affect cardiac lipid accumulation and expression of dSREBP target genes (Lim et al., 2011), strengthening links between phospholipids and regulation of SREBP-1 orthologs.

Activation of SBP-1/SREBP-1 in Response to Low PC: An Alternative to Cholesterol-Based Regulatory Mechanisms

Activation of SREBPs involves the ER, where full-length SREBP precursors are stored, and the Golgi, housing the SREBP-activating proteases S1P and S2P. Our data suggest that changes in PC levels may alter membrane function leading to SREBP-1 activation. ER stress has previously been linked to SREBP activation (Hotamisligil, 2010) and recently to PC/PE ratios in leptin-deficient, *ob/ob* mice (Fu et al., 2011). The ER-stress inducer ATF-6 is regulated similarly to SREBPs (Ye et al., 2000), thus ATF-6 could also be activated if S1P and S2P lose Golgi-specific localization. However, our data suggest that ER stress responses may occur in parallel to SBP-1 activation because stimulating the ER stress response was not sufficient to increase SBP-1 activity (Figure S3E; data not shown). Therefore, we conclude that SBP-1 activation mechanisms in response to low PC are likely independent of ER stress responses.

Elegant studies have shown that Golgi and ER separation is crucial for SREBP regulation (Bartz et al., 2008; DeBose-Boyd et al., 1999). In these studies, cells were treated with BFA, which disrupts Golgi function by inhibiting ARF-GTPase cycles essential for protein sorting in COPI-dependent Golgi-to-ER retrograde transport (Mansour et al., 1999; Peyroche et al., 1999). When cells are treated with BFA, S1 and S2 proteases collect in the ER (Bartz et al., 2008; DeBose-Boyd et al., 1999), activating SREBP-2. We have found that availability of methyl donors or PC also alters localization of S1P and S2P (Figures 6B, 6C, S5B, and S5C) and increases in mature, nuclear SREBP-1 (Figures 4C, 4E, S4B, and S4C). Intriguingly, lowering membrane PC content and BFA treatment are both predicted to inhibit ARF-GTPase cycles, although by different mechanisms. BFA binds ARF-GDP, preventing formation of active GTP-bound ARF (Donaldson and Lippincott-Schwartz, 2000). Membranes with low PC/PE ratios exhibit increased curvature (Lev, 2006), activating the ARF-GTPase repressor ARF-GAP (Bigay et al., 2003). In support of this model, S2P moved from Golgi to the ER when an ARF-activating factor, GBF1, was depleted (Citterio et al., 2008). Importantly, similar to depletion of PC synthesis enzymes (Figure 6D), we have found that depletion of GBF1 also causes SREBP-1 nuclear accumulation, showing that alterations in ARF-GTPase cycles are sufficient to activate SREBP-1. Taken together, these data suggest a simple mechanism for increasing SREBP-1 processing when membrane PC is limiting; increased curvature of the membrane may affect ARF signaling, deregulate COPI transport, and shift the distribution of S1P or S2P toward the ER, where they cleave and activate SREBP-1. Intriguingly, we found that SREBP-2 was not affected by this PC-based activation mechanism (Figures 4G and S4D), although it is activated by BFA (DeBose-Boyd et al., 1999), suggesting the possibility that SREBP-1 and SREBP-2 precursors may respond differently to these cues.

Phosphatidylcholine, 1CC Metabolism, and Links to Hepatic Lipogenesis

Lipid accumulation in the liver (hepatosteatosis) is an early step in nonalcoholic fatty liver disease (NAFLD) (Browning and Horton, 2004) and appears to predispose to subsequent, more severe pathological changes (Browning and Horton, 2004; Li et al., 2006). Although hepatic lipid accumulation may be driven by SREBP-1c in response to high insulin levels, as seen in metabolic syndrome models (Browning and Horton, 2004; Ferré and Foufelle, 2010), it may also occur when dietary or genetic lesions alter 1C metabolism or SAMe production or decrease PC levels (Larter and Yeh, 2008; Mato et al., 2008). PEMT polymorphisms, and a reduced PC/PE ratio, have also been associated with NAFLD in humans (Li et al., 2006; Song et al., 2005). When PC biosynthesis is limited in mice, hepatosteatosis is not concurrent with insulin resistance ($Ct\alpha^{-/-}$) (Jacobs et al., 2004), and $Pemt^{-/-}$ mice in fact exhibit increased insulin sensitivity (Jacobs et al., 2010), suggesting that the excess lipid production when PC is limiting is not linked to SREBP-1c upregulation as a function of insulin resistance. Unlike insulin- or oxysterol-dependent effects on SREBP-1c function (Osborne and Espenshade, 2009), the PC-linked increases are not accompanied by upregulation of the *SREBF1* transcript. This indicates that lower levels of PC resulting from diminished methylation capacity act by promoting SREBP-1 processing.

Our data suggest that the increase in nuclear SREBP-1 levels in response to limiting PC may promote elevated lipogenesis and contribute to steatosis in early stages of fatty liver diseases. Indeed, increased hepatic lipids are associated with diverse conditions such as intravenous (parenteral) feeding (Buchman et al., 1995), cystic fibrosis-associated liver disease (Colombo et al., 1998), or excess alcohol consumption (Kharbanda, 2009), in which dietary availability, absorption, or metabolism of choline and/or other 1CC metabolites could be affected. Choline supplementation can reverse hepatic lipid accumulation associated with total parenteral feeding (Buchman et al., 1995) and improve abnormal 1CC metabolite plasma levels in cystic fibrosis patients (Innis et al., 2007). Our results provide a mechanistic rationale for further exploring choline and SAMe supplementation as treatments for fatty liver diseases in humans.

To conclude, we propose a model where SBP-1/SREBP-1 is part of a conserved feedback loop responding to PC levels to

regulate expression of 1CC biogenesis genes and ensure adequate SAMe levels for PC production. Activation of other SBP-1/SREBP-1 targets in fatty acid biosynthesis pathways may also occur concomitantly, driving TAG production when PC levels are chronically low. Thus, abrogated PC feedback could be a major contributor to SREBP-1-dependent lipogenesis when methyl group metabolism is compromised by diet or genetics and predispose to hepatic lipid accumulation and fatty liver disease.

EXPERIMENTAL PROCEDURES

The Supplemental Information includes Extended Experimental Procedures. *C. elegans* strains, RNAi protocols, dietary rescue, and COPAS biosorting procedures are presented. Also included are cell culture conditions and antibodies.

C. elegans: Whole-Genome Analysis

Synchronized larvae from control and *sbp-1* RNAi cultures were harvested and RNA was isolated. cDNA was produced and hybridized to Affymetrix *C. elegans* arrays. Responsive genes were defined as having a greater than 2-fold change.

C. elegans: Metabolite Analysis

Replicates of synchronized L4/young adult *C. elegans* cultures from control or *sams-1* RNAi treatment were harvested, frozen in liquid N2, and analyzed by Metabolon. The unbiased global metabolic profiling platform utilized three independent instrument platforms: ultrahigh performance liquid chromatography/tandem mass spectrometry (UHPLC/MS/MS) optimized for basic species, UHPLC/MS/MS optimized for acidic species, and gas chromatography/mass spectrometry (GC/MS). The platform is described in detail in a previous publication (Evans et al., 2009). Briefly, samples were homogenized in a fixed ratio of water (sample amount/volume of water) then extracted using an automated MicroLab STAR system (Hamilton Company) in a fixed ratio (sample amount/volume) of methanol containing recovery standards. The resulting extract was split for analysis on the three platforms, and ion features were matched against platform-specific compound chemical libraries. UHPLC/MS utilized a Waters Acquity UPLC (Waters Corporation) coupled to an LTQ mass spectrometer (Thermo-Fisher Scientific Inc.) equipped with an electrospray ionization source. Two separate UHPLC/MS injections were performed for each sample: one optimized for positive ions and one for negative ions. Derivatized samples for GC/MS were analyzed on a Thermo-Finnigan Trace DSQ fast-scanning single-quadrupole MS operated at unit mass resolving power. Chromatographic separation, followed by full scan mass spectra, was preformed to record retention time, molecular weight (m/z), and MS/MS of all detectable ions present in the samples. Metabolites were identified by automated searching to compare ion features in experimental samples to a reference library of chemical standard entries that included retention time, molecular weight (m/z), preferred adducts, and in-source fragments, as well as their associated MS/M spectra. This library match procedure allowed rapid identification of metabolites in the experimental samples with high confidence. Comparison of experimental samples to process blanks (water only) and solvent blanks allowed automated removal of artifactual peaks.

Missing values for a given metabolite were assigned the observed minimum detected value, based on the assumption that the missing values were below the limits of detection. For the convenience of graphical visualization, the raw area counts for each metabolite were rescaled by dividing each sample value by the median observed value (excluding imputed values) for the specific metabolite. Statistical analysis was performed using "R" (http://cran.r-project.org/), a freely available open-source software package. A log transformation was applied to the observed relative concentrations for each biochemical because the variance generally increased as a function of each biochemical's average response. Welch's t tests, a variation of Student's t test for samples with unequal variances, were performed to compare data obtained between experimental groups in the study. The false-positive rate associated with multiple comparisons was calculated using the false discovery rate (FDR) method of Storey and Tibshirani (2003); q values for all tests were provided to the client.

C. elegans: Lipid Measurements

Lipids extraction, separation, and quantification (modified from Watts and Browse, 2006) were as follows: Worms were grown for 4 days starting from isolated early embryos plated on NGM plates. Lipids were extracted from frozen worm pellets with (10:10:1) chloroform/methanol/formic acid at −20° for at least 12 hr. The extract was washed with 0.2 M H_3PO_4, 1 M KCl. Lipids were recovered in the chloroform phase, dried under N_2, and redissolved in chloroform containing 0.01% BHT. Individual lipids were purified from the extracts by one-dimensional thin layer chromatography. Neutral lipids were separated on silica gel HL plates (Analtech) using 80:20:3 hexane/diethyl ether/acetic acid solvent mixture. Polar lipids were separated using a 65:43:3:2.6 chloroform/methanol/water/acetic acid solvent mixture. Separated lipids were visualized using 0.05% primuline dissolved in 80% acetone, compared to authentic standards and scraped immediately for fatty-acid methyl ester derivatization. The internal standard (15:0) was added prior to esterification. Fatty-acid methyl esters were prepared with 2.5% methanolic H_2SO_4 for analysis by gas chromatography (Watts and Browse, 2002). The relative amounts of phosphatidylcholine, phosphatidylethanolamine, and triacylglycerols were determined based on the relative amounts of fatty acids detected in each lipid fraction.

C. elegans: Dietary Rescue or Drug Treatment

For dietary rescue experiments in RNAi knockdown experiments, animals were hatched onto RNAi or control plates. On the day animals reached the L4 stage, they were washed off into S-basal media supplemented with RNAi bacteria and varying amounts of choline in 6-well plates. Plates were placed on rotators at 20°C for 18 hr before harvesting.

Cell Culture and siRNA

For analysis of gene expression in HEK293T cells (cultured as in Walker et al., 2010), SREBP-1a was transfected by Lipofectamine 2000 (Life Technologies), and cells were harvested after 48 hr. For gene knockdown in HepG2 cells, siRNA Smartpools (Thermo-Fisher Scientific) were transfected by Amaxa Nucleofector (Lonza), and cells were placed in 1% lipid-depleted serum, then harvested after 24 hr.

Immunohistochemistry or Staining with Lipid-Soluble Dyes

Antibody staining of SREBPs in cultured cells and *C. elegans* Sudan Black staining were performed as in Walker et al. (2010). S1P and S2P antibody staining were performed as in Bartz et al. (2008). For Oil Red O staining, cells were transfected with siRNA oligonucleotides by Amaxa Nucleofector and placed in 1% lipid-depleted serum. After 24 hr, cells were fixed, stained with Oil Red O for 10 min, and visualized. Microscopy for immunostaining and Oil Red O staining was performed on an Olympus ix81. Montages of images deconvolved by Nearest Neighbor algorithms were further processed by Adobe Photoshop.

Animal Handling and Liver Extract Preparation

Male liver-specific *Ctα* knockout and control mice (12 weeks old) were given free access to the high-fat diet (Bioserve, #F3282) for 3 days. Liver samples were collected from fed animals and either processed for immunoblotting with antibodies to SREBP or into Tri-reagent (Sigma) for RNA isolation. All procedures were approved by the University of Alberta's Institutional Animal Care Committee in accordance with guidelines of the Canadian Council on Animal Care.

mRNA Isolation and qPCR

mRNA was extracted by Tri-reagent (Sigma). cDNA was made from total RNA with a Transcriptor cDNA synthesis kit (Roche). qPCR was run on a Roche 480 light cycler. Duplicate samples from at least three biologically independent experiments were analyzed. Statistical significance was determined by calculating standard deviation (SD) and Student's t test. For mRNA isolation from mouse liver, after homogenization in Tri-reagent, RNA was further purified by RNAeasy columns (QIAGEN) before proceeding to cDNA synthesis and qPCR as above.

SUPPLEMENTAL INFORMATION

Supplemental information includes Extended Experimental Procedures, five figures, and one table and can be found with this article online at doi:10.1016/j.cell.2011.09.045.

ACKNOWLEDGMENTS

We thank T. Keith Blackwell for advice on examining ER stress in *C. elegans* as well as members of the Näär lab and Drs. Nick Dyson, Johnathan Whetstine, Andrew Gladden, and Tom Rapoport for helpful discussions. We express our gratitude to Drs. Stefan Taubert and Raul Mostoslavsky for critical reading of the manuscript. We thank Dr. Michael Brown for the SRD13A, SCAP-deficient cells and Dr. Joachim Seemann for advice on S1P staining. We thank the *Caenorhabditis* Genetics Center for strains. Funding for A.K.W. was provided by the Claflin Distinguished Scholar Award and R01DK084352. Funding for A.M.N. was provided by The Paul F. Glenn Laboratories for the Biological Mechanisms of Aging at Harvard Medical School and the following grants from NIH: R01DK078332 and R01GM071449. Funding for J.L.W. was provided by NIH grant R01DK074114. Funding for research in the D.E.V. and R.L.J. labs was from the Canadian Institutes of Health Research (MOP 5182 and 4487).

Received: January 26, 2011
Revised: June 14, 2011
Accepted: September 19, 2011
Published online: October 27, 2011

REFERENCES

Ashrafi, K., Chang, F.Y., Watts, J.L., Fraser, A.G., Kamath, R.S., Ahringer, J., and Ruvkun, G. (2003). Genome-wide RNAi analysis of *Caenorhabditis elegans* fat regulatory genes. Nature *421*, 268–272.

Bartz, R., Sun, L.P., Bisel, B., Wei, J.H., and Seemann, J. (2008). Spatial separation of Golgi and ER during mitosis protects SREBP from unregulated activation. EMBO J. *27*, 948–955.

Bigay, J., Gounon, P., Robineau, S., and Antonny, B. (2003). Lipid packing sensed by ArfGAP1 couples COPI coat disassembly to membrane bilayer curvature. Nature *426*, 563–566.

Brendza, K.M., Haakenson, W., Cahoon, R.E., Hicks, L.M., Palavalli, L.H., Chiapelli, B.J., McLaird, M., McCarter, J.P., Williams, D.J., Hresko, M.C., and Jez, J.M. (2007). Phosphoethanolamine N-methyltransferase (PMT-1) catalyses the first reaction of a new pathway for phosphocholine biosynthesis in *Caenorhabditis elegans*. Biochem. J. *404*, 439–448.

Brown, M.S., and Goldstein, J.L. (1997). The SREBP pathway: regulation of cholesterol metabolism by proteolysis of a membrane-bound transcription factor. Cell *89*, 331–340.

Browning, J.D., and Horton, J.D. (2004). Molecular mediators of hepatic steatosis and liver injury. J. Clin. Invest. *114*, 147–152.

Buchman, A.L., Dubin, M.D., Moukarzel, A.A., Jenden, D.J., Roch, M., Rice, K.M., Gornbein, J., and Ament, M.E. (1995). Choline deficiency: a cause of hepatic steatosis during parenteral nutrition that can be reversed with intravenous choline supplementation. Hepatology *22*, 1399–1403.

Calfon, M., Zeng, H., Urano, F., Till, J.H., Hubbard, S.R., Harding, H.P., Clark, S.G., and Ron, D. (2002). IRE1 couples endoplasmic reticulum load to secretory capacity by processing the XBP-1 mRNA. Nature *415*, 92–96.

Citterio, C., Vichi, A., Pacheco-Rodriguez, G., Aponte, A.M., Moss, J., and Vaughan, M. (2008). Unfolded protein response and cell death after depletion of brefeldin A-inhibited guanine nucleotide-exchange protein GBF1. Proc. Natl. Acad. Sci. USA *105*, 2877–2882.

Colombo, C., Battezzati, P.M., Strazzabosco, M., and Podda, M. (1998). Liver and biliary problems in cystic fibrosis. Semin. Liver Dis. *18*, 227–235.

DeBose-Boyd, R.A., Brown, M.S., Li, W.P., Nohturfft, A., Goldstein, J.L., and Espenshade, P.J. (1999). Transport-dependent proteolysis of SREBP: relocation of site-1 protease from Golgi to ER obviates the need for SREBP transport to Golgi. Cell *99*, 703–712.

Dobrosotskaya, I.Y., Seegmiller, A.C., Brown, M.S., Goldstein, J.L., and Rawson, R.B. (2002). Regulation of SREBP processing and membrane lipid production by phospholipids in *Drosophila*. Science *296*, 879–883.

Donaldson, J.G., and Lippincott-Schwartz, J. (2000). Sorting and signaling at the Golgi complex. Cell *101*, 693–696.

Evans, A.M., DeHaven, C.D., Barrett, T., Mitchell, M., and Milgram, E. (2009). Integrated, nontargeted ultrahigh performance liquid chromatography/electrospray ionization tandem mass spectrometry platform for the identification and relative quantification of the small-molecule complement of biological systems. Anal. Chem. *81*, 6656–6667.

Ferré, P., and Foufelle, F. (2010). Hepatic steatosis: a role for de novo lipogenesis and the transcription factor SREBP-1c. Diabetes Obes. Metab. *12* (Suppl 2), 83–92.

Fu, S., Yang, L., Li, P., Hofmann, O., Dicker, L., Hide, W., Lin, X., Watkins, S.M., Ivanov, A.R., and Hotamisligil, G.S. (2011). Aberrant lipid metabolism disrupts calcium homeostasis causing liver endoplasmic reticulum stress in obesity. Nature *473*, 528–531.

Guo, Y., Walther, T.C., Rao, M., Stuurman, N., Goshima, G., Terayama, K., Wong, J.S., Vale, R.D., Walter, P., and Farese, R.V. (2008). Functional genomic screen reveals genes involved in lipid-droplet formation and utilization. Nature *453*, 657–661.

Hagen, R.M., Rodriguez-Cuenca, S., and Vidal-Puig, A. (2010). An allostatic control of membrane lipid composition by SREBP1. FEBS Lett. *584*, 2689–2698.

Hansen, M., Hsu, A.L., Dillin, A., and Kenyon, C. (1995). New genes tied to endocrine, metabolic and dietary regulation of lifespan from a *Caenorhabditis elegans* RNAi screen. PLoS Genet. *1*, 119–128.

Horton, J.D., Bashmakov, Y., Shimomura, I., and Shimano, H. (1998). Regulation of sterol regulatory element binding proteins in livers of fasted and refed mice. Proc. Natl. Acad. Sci. USA *95*, 5987–5992.

Horton, J.D., Goldstein, J.L., and Brown, M.S. (2002). SREBPs: activators of the complete program of cholesterol and fatty acid synthesis in the liver. J. Clin. Invest. *109*, 1125–1131.

Hotamisligil, G.S. (2010). Endoplasmic reticulum stress and the inflammatory basis of metabolic disease. Cell *140*, 900–917.

Hua, X., Nohturfft, A., Goldstein, J.L., and Brown, M.S. (1996). Sterol resistance in CHO cells traced to point mutation in SREBP cleavage-activating protein. Cell *87*, 415–426.

Innis, S.M., Davidson, A.G., Melynk, S., and James, S.J. (2007). Choline-related supplements improve abnormal plasma methionine-homocysteine metabolites and glutathione status in children with cystic fibrosis. Am. J. Clin. Nutr. *85*, 702–708.

Jacobs, R.L., Devlin, C., Tabas, I., and Vance, D.E. (2004). Targeted deletion of hepatic CTP:phosphocholine cytidylyltransferase alpha in mice decreases plasma high density and very low density lipoproteins. J. Biol. Chem. *279*, 47402–47410.

Jacobs, R.L., Stead, L.M., Devlin, C., Tabas, I., Brosnan, M.E., Brosnan, J.T., and Vance, D.E. (2005). Physiological regulation of phospholipid methylation alters plasma homocysteine in mice. J. Biol. Chem. *280*, 28299–28305.

Jacobs, R.L., Lingrell, S., Zhao, Y., Francis, G.A., and Vance, D.E. (2008). Hepatic CTP:phosphocholine cytidylyltransferase-alpha is a critical predictor of plasma high density lipoprotein and very low density lipoprotein. J. Biol. Chem. *283*, 2147–2155.

Jacobs, R.L., Zhao, Y., Koonen, D.P., Sletten, T., Su, B., Lingrell, S., Cao, G., Peake, D.A., Kuo, M.S., Proctor, S.D., et al. (2010). Impaired de novo choline synthesis explains why phosphatidylethanolamine N-methyltransferase-deficient mice are protected from diet-induced obesity. J. Biol. Chem. *285*, 22403–22413.

Kharbanda, K.K. (2009). Alcoholic liver disease and methionine metabolism. Semin. Liver Dis. *29*, 155–165.

Larter, C.Z., and Yeh, M.M. (2008). Animal models of NASH: getting both pathology and metabolic context right. J. Gastroenterol. Hepatol. *23*, 1635–1648.

Lev, S. (2006). Lipid homeostasis and Golgi secretory function. Biochem. Soc. Trans. *34*, 363–366.

Li, Z., Agellon, L.B., Allen, T.M., Umeda, M., Jewell, L., Mason, A., and Vance, D.E. (2006). The ratio of phosphatidylcholine to phosphatidylethanolamine influences membrane integrity and steatohepatitis. Cell Metab. *3*, 321–331.

Lim, H.Y., Wang, W., Wessells, R.J., Ocorr, K., and Bodmer, R. (2011). Phospholipid homeostasis regulates lipid metabolism and cardiac function through SREBP signaling in Drosophila. Genes Dev. *25*, 189–200.

Lu, S.C., Alvarez, L., Huang, Z.Z., Chen, L., An, W., Corrales, F.J., Avila, M.A., Kanel, G., and Mato, J.M. (2001). Methionine adenosyltransferase 1A knockout mice are predisposed to liver injury and exhibit increased expression of genes involved in proliferation. Proc. Natl. Acad. Sci. USA *98*, 5560–5565.

Mansour, S.J., Skaug, J., Zhao, X.H., Giordano, J., Scherer, S.W., and Melançon, P. (1999). p200 ARF-GEP1: a Golgi-localized guanine nucleotide exchange protein whose Sec7 domain is targeted by the drug brefeldin A. Proc. Natl. Acad. Sci. USA *96*, 7968–7973.

Mato, J.M., and Lu, S.C. (2005). Homocysteine, the bad thiol. Hepatology *41*, 976–979.

Mato, J.M., Martínez-Chantar, M.L., and Lu, S.C. (2008). Methionine metabolism and liver disease. Annu. Rev. Nutr. *28*, 273–293.

McKay, R.M., McKay, J.P., Avery, L., and Graff, J.M. (2003). *C. elegans:* a model for exploring the genetics of fat storage. Dev. Cell *4*, 131–142.

Osborne, T.F., and Espenshade, P.J. (2009). Evolutionary conservation and adaptation in the mechanism that regulates SREBP action: what a long, strange tRIP it's been. Genes Dev. *23*, 2578–2591.

Palavalli, L.H., Brendza, K.M., Haakenson, W., Cahoon, R.E., McLaird, M., Hicks, L.M., McCarter, J.P., Williams, D.J., Hresko, M.C., and Jez, J.M. (2006). Defining the role of phosphomethylethanolamine N-methyltransferase from *Caenorhabditis elegans* in phosphocholine biosynthesis by biochemical and kinetic analysis. Biochemistry *45*, 6056–6065.

Peyroche, A., Antonny, B., Robineau, S., Acker, J., Cherfils, J., and Jackson, C.L. (1999). Brefeldin A acts to stabilize an abortive ARF-GDP-Sec7 domain protein complex: involvement of specific residues of the Sec7 domain. Mol. Cell *3*, 275–285.

Seegmiller, A.C., Dobrosotskaya, I., Goldstein, J.L., Ho, Y.K., Brown, M.S., and Rawson, R.B. (2002). The SREBP pathway in *Drosophila:* regulation by palmitate, not sterols. Dev. Cell *2*, 229–238.

Shen, X., Ellis, R.E., Sakaki, K., and Kaufman, R.J. (2005). Genetic interactions due to constitutive and inducible gene regulation mediated by the unfolded protein response in C. elegans. PLoS Genet. *1*, e37.

Song, J., da Costa, K.A., Fischer, L.M., Kohlmeier, M., Kwock, L., Wang, S., and Zeisel, S.H. (2005). Polymorphism of the PEMT gene and susceptibility to nonalcoholic fatty liver disease (NAFLD). FASEB J. *19*, 1266–1271.

Storey, J.D., and Tibshirani, R. (2003). Statistical significance for genomewide studies. Proc. Natl. Acad. Sci. USA *100*, 9440–9445.

Testerink, N., van der Sanden, M.H., Houweling, M., Helms, J.B., and Vaandrager, A.B. (2009). Depletion of phosphatidylcholine affects endoplasmic reticulum morphology and protein traffic at the Golgi complex. J. Lipid Res. *50*, 2182–2192.

Vance, D.E., Li, Z., and Jacobs, R.L. (2007). Hepatic phosphatidylethanolamine N-methyltransferase, unexpected roles in animal biochemistry and physiology. J. Biol. Chem. *282*, 33237–33241.

Vance, J.E., and Vance, D.E. (2004). Phospholipid biosynthesis in mammalian cells. Biochem. Cell Biol. *82*, 113–128.

Walker, A.K., Yang, F., Jiang, K., Ji, J.Y., Watts, J.L., Purushotham, A., Boss, O., Hirsch, M.L., Ribich, S., Smith, J.J., et al. (2010). Conserved role of SIRT1 orthologs in fasting-dependent inhibition of the lipid/cholesterol regulator SREBP. Genes Dev. *24*, 1403–1417.

Watkins, S.M., Zhu, X., and Zeisel, S.H. (2003). Phosphatidylethanolamine-N-methyltransferase activity and dietary choline regulate liver-plasma lipid flux and essential fatty acid metabolism in mice. J. Nutr. *133*, 3386–3391.

Watts, J.L., and Browse, J. (2002). Genetic dissection of polyunsaturated fatty acid synthesis in *Caenorhabditis elegans*. Proc. Natl. Acad. Sci. USA *99*, 5854–5859.

Watts, J.L., and Browse, J. (2006). Dietary manipulation implicates lipid signaling in the regulation of germ cell maintenance in *C. elegans*. Dev. Biol. *292*, 381–392.

Yang, F., Vought, B.W., Satterlee, J.S., Walker, A.K., Jim Sun, Z.Y., Watts, J.L., DeBeaumont, R., Saito, R.M., Hyberts, S.G., Yang, S., et al. (2006). An ARC/Mediator subunit required for SREBP control of cholesterol and lipid homeostasis. Nature *442*, 700–704.

Ye, J., Rawson, R.B., Komuro, R., Chen, X., Davé, U.P., Prywes, R., Brown, M.S., and Goldstein, J.L. (2000). ER stress induces cleavage of membrane-bound ATF6 by the same proteases that process SREBPs. Mol. Cell *6*, 1355–1364.

Zeisel, S.H. (2008). Genetic polymorphisms in methyl-group metabolism and epigenetics: lessons from humans and mouse models. Brain Res. *1237*, 5–11.

Note Added in Proof

While our study was under review, Li et al. also found that *sams-1* and *pmt-1* deficiencies produced lipid accumulation in *C. elegans*: Li, Y., Na, K., Lee, H.J., Lee, E.Y., and Paik, Y.K. (2011). Contribution of *sams-1* and *pmt-1* to lipid homeostasis in adult *Caenorhabditis elegans*. J. Biochem. *149*, 529–538.

Cell

EXTENDED EXPERIMENTAL PROCEDURES

C. elegans

Strains used were N2, CE458, and RT1315. RNAi and analysis of GFP::SBP-1, *sbp-1(ep79)* were performed as in Walker et al. (2010).

Quantification of *pfat-7*::GFP Expression

Gravid adults of the p*fat-7*::GFP (*rtIs30*) carrying strain HA1842 (UV-integrated from strain BC15777, 3 times outcrossed) were treated with bleach and eggs were allowed to hatch in M9 overnight at 20°C. 100–200 L1 larvae were then added per well in a 96-well plate with S-complete medium and fed with bacteria containing empty vector (L4440) or RNAi clones of interest. Worms were allowed to grow to adulthood at 20°C for 3 days. GFP intensity and length of the worms were then measured for each well by the COPAS Select flow sorter (Union Biometrica). Data points with a "time of flight value" (TOF, length) larger than or equal to 150 and a "green channel value" (GFP intensity) larger than or equal to 50 were considered to be worms. Fold change of GFP intensity was calculated for each RNAi clone compared to worms fed with empty vector bacteria.

Cell Culture

For experiments in HepG2 cells, cultures were maintained in MEM supplemented with 10% fetal calf serum, penicillin/streptomycin, L-glutamine, and sodium pyruvate. For experiments in SRD13A, cells were maintained in 8.5% CO_2 in a humidified atmosphere. Cells were grown in HamF12/DMEM in 5% FCS, supplemented with oleic acid, cholesterol, and mevalonate. Cells were selected weekly with Amphotericin. siRNA oligos were designed to target hamster *Ct*α, sequences are available upon request.

Immunoblot Analysis

Cells were lysed in High Salt RIPA (50 mM Tris, pH 7.4; 400 mM NaCl; 0.1% SDS; 0.5% NaDeoxycholate; 1% NP-40). Extracts were run out on Novex Bis-Tris gels (Invitrogen) and blotted onto nitrocellulose (Biorad). Antibodies used were as follows: SREBP-1a m2121 (Millipore), SREBP-2 (Abcam), Giantin (Abcam) (Shiba et al., 2010), α-mannosidase II (Chang et al., 2005), (Abcam), Site-1 protease, Site-2 protease (Abcam), KDEL, (HDEL, Santa Cruz).

Clustering Analysis of *sbp-1*-Responsive Genes in *C. elegans*

Hierarchical clustering was performed as in Shioda et al. (2006) and Walker et al. (2010). Both genes and arrays were centered to the medians and subjected to two-dimensional average linkage clustering with uncentered correlation for similarity metric.

SUPPLEMENTAL REFERENCES

Chang, P., Coughlin, M., and Mitchison, T.J. (2005). Tankyrase-1 polymerization of poly(ADP-ribose) is required for spindle structure and function. Nat. Cell Biol. *7*, 1133–1139.

Shiba, Y., Römer, W., Mardones, G.A., Burgos, P.V., Lamaze, C., and Johannes, L. (2010). AGAP2 regulates retrograde transport between early endosomes and the TGN. J. Cell Sci. *123*, 2381–2390.

Shioda, T., Chesnes, J., Coser, K.R., Zou, L., Hur, J., Dean, K.L., Sonnenschein, C., Soto, A.M., and Isselbacher, K.J. (2006). Importance of dosage standardization for interpreting transcriptomal signature profiles: evidence from studies of xenoestrogens. Proc. Natl. Acad. Sci. USA *103*, 12033–12038.

Walker, A.K., Yang, F., Jiang, K., Ji, J.Y., Watts, J.L., Purushotham, A., Boss, O., Hirsch, M.L., Ribich, S., Smith, J.J., et al. (2010). Conserved role of SIRT1 orthologs in fasting-dependent inhibition of the lipid/cholesterol regulator SREBP. Genes Dev. *24*, 1403–1417.

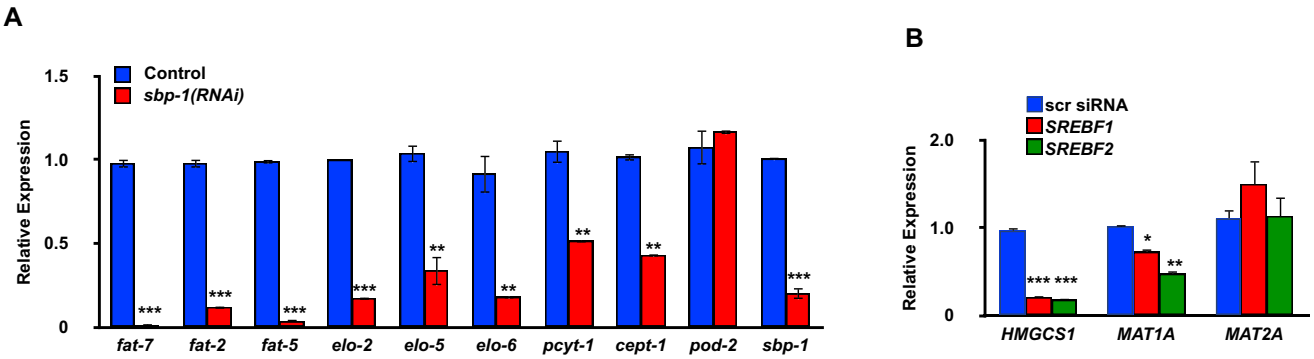

Figure S1. Transcriptional Control of Multiple Metabolic Pathways by SBP-1, Related to Figure 1

(A) SBP-1 regulates a broad subset of genes involved in fatty-acid biogenesis and phospholipid production in *C. elegans,* as shown by qRT-PCR analysis. Error bars represent SD; statistical relevance, p value < 0.05 shown by (*), p value < 0.001 shown by (**), p value < 0.001 shown by (***).

(B) Analysis of human HeLa S cells by qRT-PCR after short-interfering RNA (siRNA) knockdown of SREBP-1a and SREBP-2 shows that expression of the 1CC gene *MAT1A* is also decreased compared to control cells transfected with a scrambled siRNA construct. *HMGCS1* was used as a positive control. Error bars show SD, statistical relevance, p value < 0.05 shown by (*), p value < 0.001 shown by (**), p value < 0.001 shown by (***).

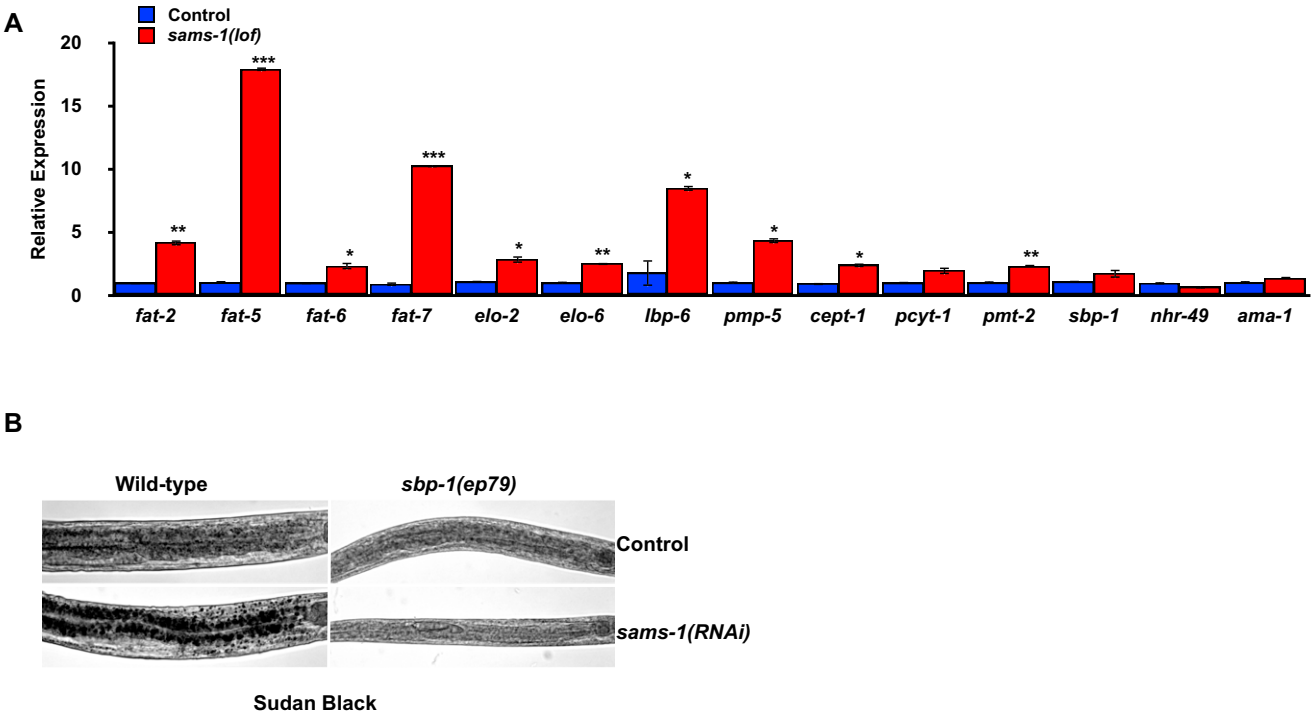

Figure S2. Gene Expression after Knockdown of an *S*-Adenosylmethionine Synthetase in *C. elegans*, Related to Figure 2

(A) qRT-PCR analysis in a *sams-1* loss-of-function (lof) allele, *sams-1(ok3033)*, shows that FA desaturase (*fat-5, -6*, and *-7*) gene expression is strongly upregulated, as in *sams-1(RNAi)*. Expression of other SBP-1-responsive genes is also elevated; however, the *sbp-1* mRNA level is not increased. Expression of housekeeping genes, such as *ama-1* (RNA Pol II large subunit) is not altered. Error bars represent SD; statistical relevance; p value < 0.05 shown by (*), p value < 0.01 shown by (**), p value < 0.001 shown by (***).

(B) Sudan Black staining shows that lipid droplets do not accumulate in animals after *sams-1* RNAi if *sbp-1* activity is also compromised.

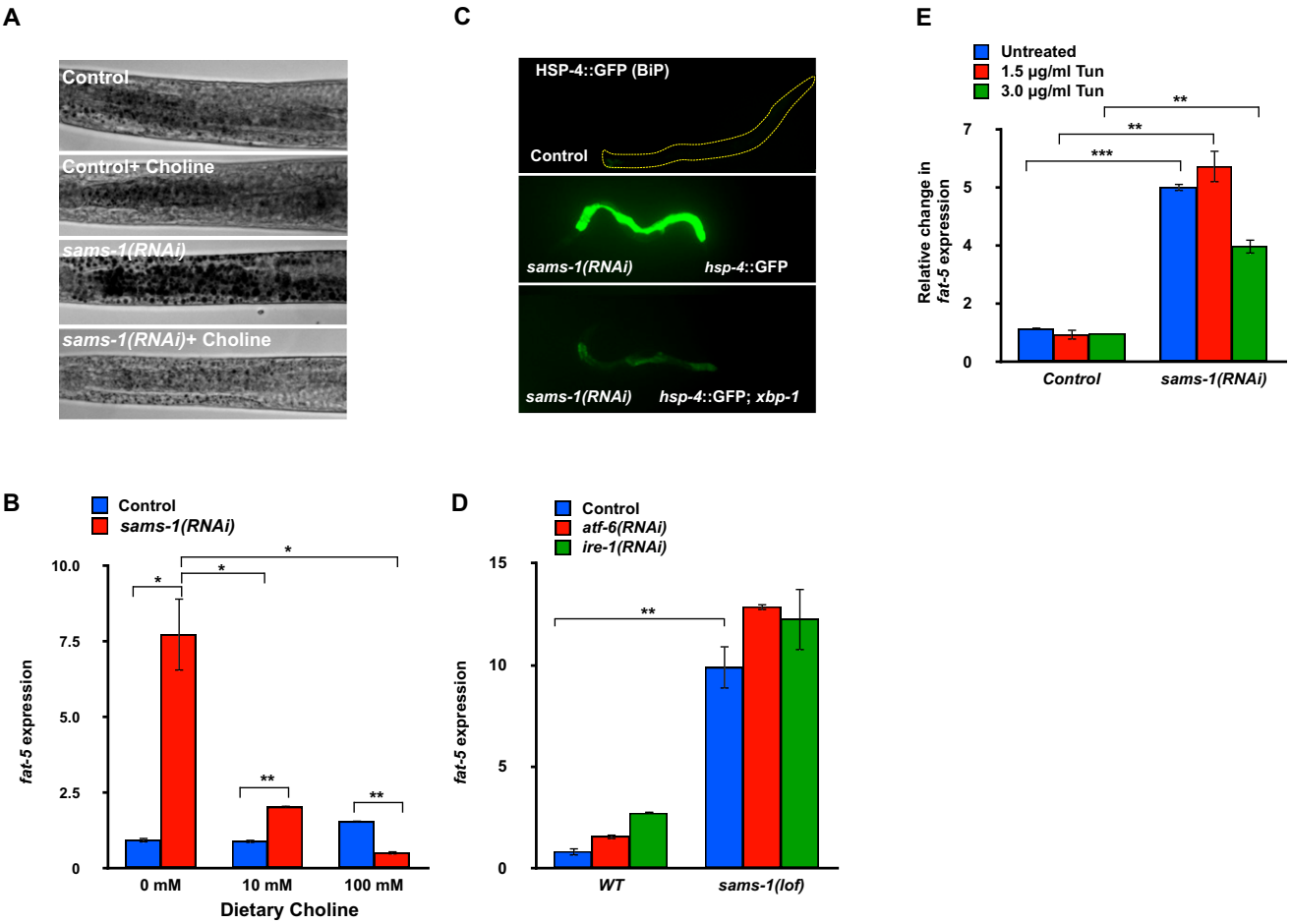

Figure S3. Rescue of *sams-1(RNAi)* or *(lof)*-Mediated Phenotypes by Choline, Related to Figure 3

(A and B) Dietary choline rescues *sams-1(RNAi)* phenotypes such as increased lipid droplet accumulation (A) and overexpression of the SBP-1-dependent target gene *fat-5* (B).

(C) The endoplasmic reticulum (ER) stress reporter *hsp-4*::GFP (Calfon et al., 2002) is activated after *sams-1(RNAi)*. This activation does not occur when the ER stress response is inhibited by deletion of *xbp-1*.

(D) Blocking the ER stress response through *atf-6* or *ire-6* RNAi does not affect upregulation of the SBP-1 target gene *fat-5* in *sams-1(lof)* animals.

(E) Expression of *fat-5* does not increase after treatment with the ER stress inducer tunicamycin. Error bars show SD. Statistical relevance (p value) is shown by <0.05, *; <0.01, **, <0.005, ***.

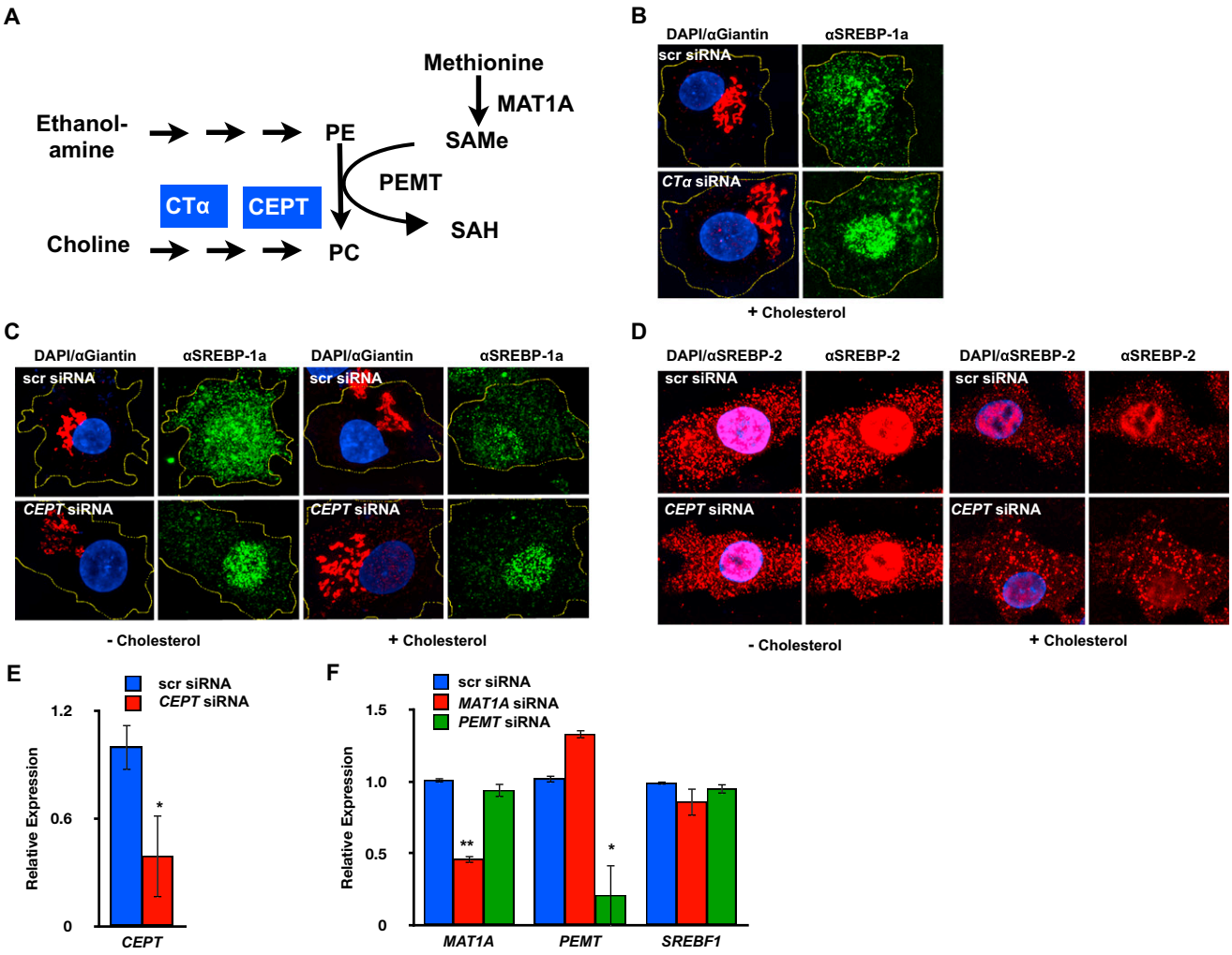

Figure S4. Effects on SREBP-1 and SREBP-2 Function in Response to Inhibition of SAMe Production and PC Biosynthesis, Related to Figure 4

(A) Schematic diagram of PC biosynthesis in mammals. Genes analyzed in subsequent figures are shown in blue boxes.

(B and C) Addition of cholesterol to lipid-depleted serum did not block the SREBP-1 nuclear accumulation after limiting PC biogenesis with *CTα* (B) or *CEPT* siRNA (C).

(D) SREBP-2 nuclear accumulation is decreased in the presence of cholesterol but not affected by *CTα* or *CEPT* knockdown.

(E and F) qRT-PCR shows that *CEPT* (E), *MAT1A*, or *PEMT* (F) mRNAs are depleted after siRNA knockdown in HepG2 cells. Error bars show SD. Statistical relevance (p value) is shown by < 0.05, *; < 0.01, **, < 0.005, ***.

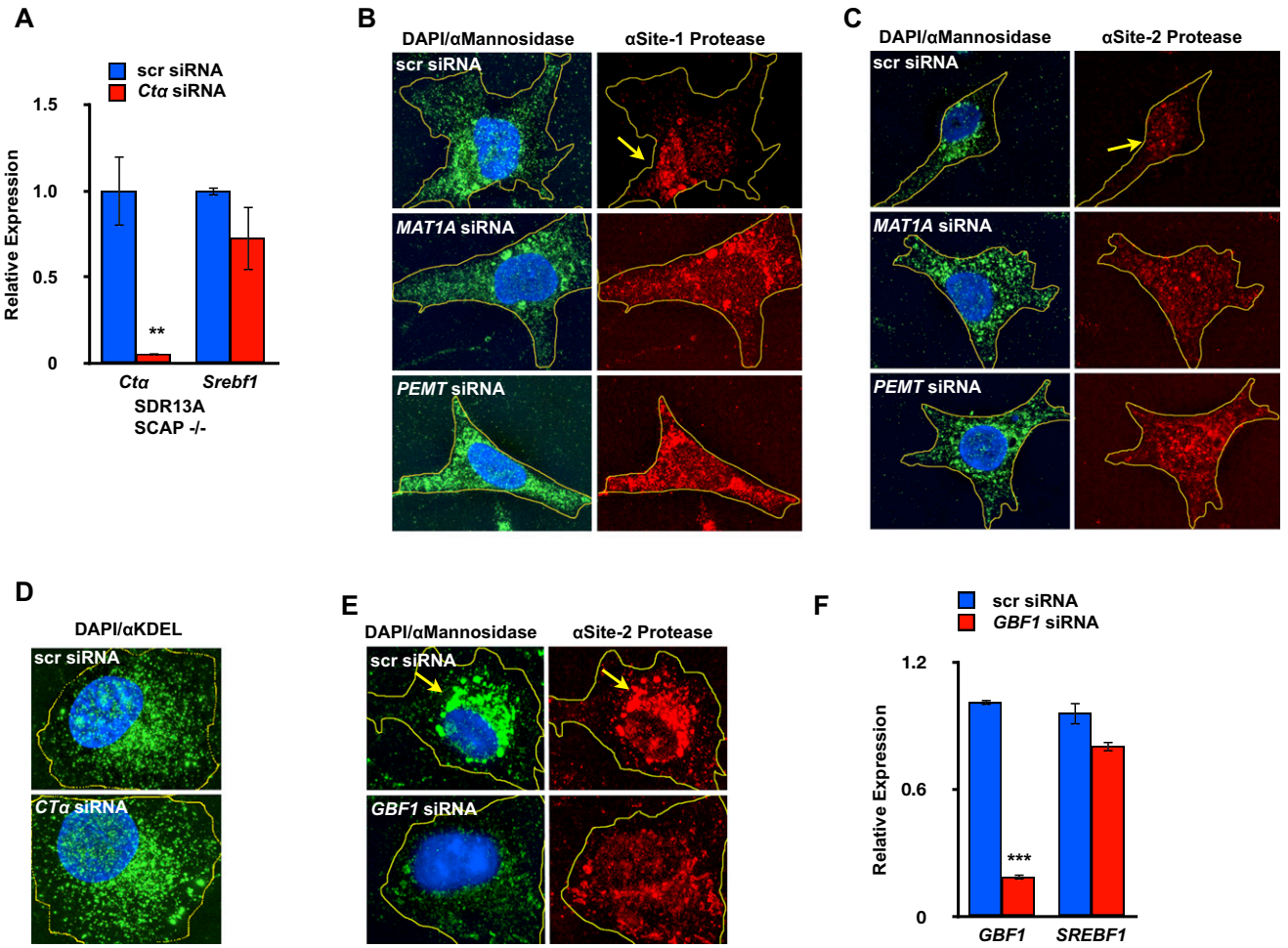

Figure S5. Effects on Localization of SREBP-Activating Proteases in Response to Inhibition of SAMe Production, PC Biosynthesis, and ER/Golgi Transport, Related to Figure 6

(A) Expression of *Ctα* is strongly decreased in SCAP$^{-/-}$ SDR13A cells in response to *Ctα* siRNA, whereas *Srebf1* expression is unchanged.

(B and C) siRNA inhibition of *MAT1A* or *PEMT* causes loss of Golgi-specific localization of SREBP-1-activating S1P (B) or S2P (C) in HepG2 cells.

(D) The ER marker KDEL stains control and *CTα* siRNA-treated HepG2 cells in a similar manner.

(E) Blocking ARF-GTPase signaling by *GBF1* RNAi in HepG2 cells causes S2P relocalization as in Citterio et al. (2008).

(F) siRNA for *GBF1* causes a decrease in its mRNA levels in HepG2 cells, whereas *SREBF1* expression is unaltered. Error bars show SD. Statistical relevance (p value) is shown by <0.05, *; <0.01, **, <0.005, ***.